1-1-2008

Studies of potential sources that contributed to atmospheric mercury in Toronto, Canada

Irene Cheng
Ryerson University

STUDIES OF POTENTIAL SOURCES THAT CONTRIBUTED TO ATMOSPHERIC MERCURY IN TORONTO, CANADA

by

Irene Cheng
Bachelor of Applied Science, Toronto, 2006

A thesis presented to Ryerson University

In partial fulfillment of the

requirements for the degree of

Master of Applied Science

in the Program of

Environmental Applied Science and Management

Toronto, Ontario, Canada, 2008

Author's Declaration Page

I hereby declare that I am the sole author of this thesis. I authorize Ryerson University to lend this thesis to other institutions or individuals for the purpose of scholarly research.

I further authorize Ryerson University to reproduce this thesis by photocopying or by other means, in total or in part, at the request of other institutions or individuals for the purpose of scholarly research.

Abstract

Studies of Potential Sources That Contributed To Atmospheric Mercury in Toronto, Canada

Master of Applied Science, 2008
Irene Cheng
Environmental Applied Science and Management
Ryerson University

The objectives of the study were to identify sources of mercury (Hg) measured in downtown Toronto, Canada using Positive Matrix Factorization (PMF), Principal Components Analysis (PCA), ratio analysis, back trajectories, and correlation analyses. Atmospheric Hg species (i.e., GEM, PHg<2.5, RGM) and air pollutants measured from December 2003 to November 2004 were the input variables. Model results suggest industrial sources (chemical production, metal production, sewage treatment), rather than coal combustion, were the major contributors to measured Hg levels. Both the PMF model and PCA identified factors that cannot be characterized using the National Pollutant Release Inventory emissions data. Correlation analyses revealed direct emissions were the sources of RGM in spring, summer and fall, and the occurrence of GEM oxidation by ozone in the summer. Elevated Hg events are attributed to emissions from regional point sources, photochemical processes involving ozone, and potentially urban sources near the sampling site.

Acknowledgements

I would like to thank my thesis supervisor, Dr. Julia Lu, for giving me the opportunity to work on this project and gain valuable research experience. I would also like to acknowledge the Ryerson Graduate Award and my teaching assistant position for the Geotechnical Properties of Soils course in the Civil Engineering Department for the additional financial support during my Master's study. Finally, I like to say thank you to my Mom and brother for their support of my university studies in the Environmental and Engineering fields.

Table of Contents

List of Tables

List of Figures

List of Abbreviations

CAMNet	Canadian Atmospheric Mercury Measurement Network
CMAQ	Community Multi-scale Air Quality
CMB	Chemical Mass Balance
EDAS	Eta Data Assimilation System
GEM	Gaseous Elemental Mercury
GIS	Geographic Information Systems
HYSPLIT	HYbrid Single-Particle Lagrangian Integrated Trajectory
MOE	Ministry of the Environment (Province of Ontario)
NCEP	National Centers for Environmental Prediction
NPRI	National Pollutant Release Inventory
PCA	Principal Components Analysis
PHg	Particulate Mercury
PHg<2.5	Particulate Mercury with an aerodynamic diameter less than 2.5 μm
$PM_{2.5}$	Fine Particulate Matter
PMF	Positive Matrix Factorization
RGM	Reactive Gaseous Mercury
TGM	Total Gaseous Mercury
USEPA	United States Environmental Protection Agency
UTC	Universal Time Coordinated
VOC	Volatile Organic Compounds

1. Introduction

1.1 Why Mercury Research?

1.1.1 Where Mercury is Found and Used

Mercury is found naturally in a mercuric sulfide mineral called cinnabar, which is ~86% mercury by weight, and in rocks and fossil fuels (Environment Canada, 2004a). Depending on the type of fossil fuel, e.g. hard coal, brown coal, crude oil, or natural gas, and the location where the excavation of the fossil fuel took place, the mercury content can vary. It ranges from 0.01-1.5 g/ton in coal, 0.01-0.5 g/ton in crude oil, and 0-5.0 mg/m^3 in natural gas (Pacyna et al., 2006). Mercury is currently being produced in Spain, North and South America and Asia (mainly in China and the countries of former USSR) (Pacyna et al., 2006) and used mainly by industries to manufacture products. Mercury is consumed in chloralkali facilities, which uses mercury electrodes to manufacture sodium hydroxide and chlorine that can be made into plastics and pesticides. It is also used in gold mining, where mercury forms an amalgam with gold in order to separate gold from the rest of the ore. Dental amalgam, which is used to fill tooth cavities, is composed of metals and mercury and has led to widespread exposure to mercury (Gochfeld, 2003). The manufacturing of fluorescent light bulbs, electrical devices, and older types of thermometers, blood pressure meters, manometers, and hydrometers also contain elemental mercury. Metallic mercury is ideal for these applications because of its unique physical properties, such as high electrical conductivity, boiling point and density. A comparison of the consumption patterns between early 1970 (peak global Hg consumption) and late 1990s in the U.S. and Sweden, shown in Table 1.1, illustrates that the consumption of mercury of various industrial activities have changed over time.

Table 1.1: The mercury consumption trends in Sweden and the United States in the early 70s and late 90s. The consumption patterns are expressed as a percent.

Industrial activities	Sweden		United States	
	Early 1970s	1996-2000	Early 1970s	1996-2000
Chloralkali and catalyst (in US)	75.1	58	23.3-24.5	30
Electrical devices and lighting	1.2	3	18.1-20.8	25
Batteries	1.3	0	11.3-24.5	0
Dental	17.3	39	3.8-5.6	10
Non-electrical instruments	0.8	0	12.4	12
Fungicides and pesticides	-	0	3.5-22.6	0
Paper industry	3.9	0	0	0

Source: Hylander and Meili (2005)

1.1.2 Mercury Emissions from Anthropogenic Sources

Despite the improvements to reduce the use of mercury, industries account for 30% of the total global anthropogenic mercury emissions, which reached 2,200 tons in 2000 (Pacyna et al., 2006). Anthropogenic sources can contribute up to 50% of the mercury emitted into the atmosphere, with the other 50% due to natural emissions from soil, vegetation, water and volcanic activity (Bash et al., 2004; Pacyna et al., 2006). However, mercury in soil, vegetation and water likely originated from the deposition of atmospheric Hg that was emitted from anthropogenic sources (Pacyna et al., 2006). Industrial emissions of mercury mainly come from gold production (248 tons), non-ferrous metal production (149 tons) and cement production (140 tons). The remaining two-thirds of the anthropogenic emissions are due to stationary combustion sources, which include coal-fired power generation and industrial/residential boilers. Pacyna et

al. (2006) reported that China (605 tons), South Africa (257 tons), India (150 tons), Japan (144 tons), Australia (124 tons) and the USA (109 tons) were the major emitters of mercury in 2000. Natural or re-emitted and anthropogenic sources of mercury are listed in Table 1.2.

Table 1.2: Types of natural and anthropogenic sources of mercury emissions

Sources of mercury	**References**
Natural sources or re-emissions	
Soil	Eckley and Branfireun (2008); Lindberg et al. (1998)
Land application of biosolids	Cobbett and Van Heyst (2007)
Water	Pirrone et al. (2001)
Vegetation	Lindberg et al. (1998)
Volcanic activity	Bagnato et al. (2007)
Mineralized areas (e.g., Hg-rich rocks and ores)	Gustin et al. (2003); Nacht et al. (2004)
Anthropogenic sources	
Stationary combustion (e.g., power plants and boilers)	Edgerton et al. (2006); Pacyna et al. (2006); Pirrone et al. (2001); Wong et al. (2006)
Oil combustion	Pacyna et al. (2006); Pirrone et al. (2001)
Cement production	Pacyna et al. (2006); Pirrone et al. (2001)
Mine wastes and tailings	Gustin et al. (2003); Nacht et al. (2004)
Metal production (e.g., Cu, Pb and Zn smelting)	Pacyna et al. (2006); Pirrone et al. (2001)
Steel production	Pacyna et al. (2006); Pirrone et al. (2001)
Chlor-alkali plants	Landis et al. (2004); Pacyna et al. (2006); Southworth et al. (2004)
Mercury production	Pacyna et al. (2006); Wong et al. (2006)
Gold production	Pacyna et al. (2006); Wong et al. (2006)
Waste disposal and incineration (e.g., municipal solid waste, sewage sludge, hazardous wastes)	Hagreen and Lourie (2004); Pacyna et al. (2006); Pirrone et al. (2001)
Production and use of Hg-containing products	Hagreen and Lourie (2004); Streets et al. (2005)
Vehicle emissions	Landis et al. (2007)
Urban pavement, roofs, and windows	Eckley and Branfireun (2008)

In Canada, the major emission sources of Hg are base metal processing facilities (2.8 tons in 2000), waste incinerators (1.2 tons in 2000) including municipal solid wastes, medical, hazardous and sewage sludge wastes, and coal-fired electric power generation plants (2.7 tons in 2003) (CCME, 2000, 2006). The use of mercury-containing products ends up in the waste

and/or metal recycling stream leading to mercury emissions from these industries (Hagreen and Lourie, 2004). Hagreen and Lourie (2004) estimated that the use and disposal of Hg-containing products release more than 2 tons of mercury into the air each year, which is comparable to the amount released from Hg point sources. Current Hg inventory indicate that mercury emissions in North America and Europe have been decreasing mainly because they have vastly reduced the production and consumption of mercury by using mercury substitutes and improving the mercury recovery process. However, the study by Pacyna et al. (2006) predicts that emissions will continue to increase in Africa and Asia due to the increasing energy demand and reliance on fossil fuels.

1.1.3 Mercury in the Atmosphere

Atmospheric mercury is operationally divided into three different forms: elemental mercury (GEM), reactive gaseous mercury (RGM) and mercury bounded to airborne particles (PHg). RGM is the divalent inorganic form of mercury (Hg (II)) that exists in the gas phase (Lindberg and Stratton, 1998). Most of the mercury emitted from point sources is in the form of GEM, but RGM can also be directly emitted from sources, such as coal combustion, due to interactions with flue gas molecules, surface of particulate matter, and/or sorbents used to capture mercury (Ralston et al., 2005; Tang et al., 2007). Comprising about 98% of the mercury in the atmosphere under normal environmental conditions (except in the polar spring after polar sunrise), GEM has the longest atmospheric residence time (e.g. 4 months to 1 year (Schroeder and Munthe, 1998)) of all the mercury species and is capable of long distance transport, e.g. globally. RGM and PHg species have shorter atmospheric residence times (e.g. hours to few weeks (Manolopoulos, 2007b)) than GEM, which means they are more likely to deposit at

distances closer to the source of emission. The atmospheric residence times of mercury species is dictated by their different physical and chemical properties as shown in Table 1.3. Elemental mercury has a higher vapour pressure than its inorganic forms, such as mercuric chloride ($HgCl_2$), at the same temperature (Schroeder and Munthe, 1998). Furthermore, RGM is 5 orders of magnitude more soluble in water than GEM (Lynam and Keeler, 2005), which increases the chance of RGM deposition. Due to its higher surface reactivity, RGM also readily adsorbs onto aerosols and particulate matter to form PHg, which are also subject to deposition.

Table 1.3: Selective physical and chemical properties of mercury

Physical state at $0^{o}C$, 1 atm	Liquid
Oxidation states	0, +1, +2; most stable forms in the atmosphere are 0 (GEM) and +2 (RGM)
Specific gravity at $20^{o}C$	13.55
Boiling point (^{o}C)	357 for Hg
Melting point (^{o}C)	-39 for Hg
Electrical resistivity at $50^{o}C$ (Ωm)	9.84×10^{-7} for Hg
Solubility in water at $20^{o}C$ (g/l)	49.4×10^{-6} for Hg; 66 for $HgCl_2$
Vapour pressure at 1 atm (Pa)	0.180 for Hg; 8.99×10^{-3} for $HgCl_2$

Sources: Schroeder and Munthe (1998); Weast and Selby (1967)

1.1.4 Mercury Transformation, Transport and Fate in the Environment

Although the background mercury levels in the ambient air (1.7 ng/m^3 reported by Ebinghaus et al. 2003) are not high enough to lead to direct human health impacts, elemental mercury can be transformed to Hg(II) (the divalent, inorganic stable form) by oxidants in the air and transported to other environmental media, such as soil, vegetation, and water, via wet and

dry deposition (Environment Canada, 2004a). Once deposited in water, sediments, and wetlands, Hg(II) can be transformed by bacteria under acidic and anaerobic conditions to methylmercury compounds, the most toxic forms of mercury to living organisms that can be bioaccumulated in the food chain (Environment Canada, 2004a).

1.1.5 Health Effects from Mercury Exposure

Human exposure to methylmercury may come from the consumption of methylmercury-contaminated fish and seafood, such as in the cases of Minamata disease in Japan, due to its ability to bioaccumulate in the aquatic food chain. It can also come from inhalation of elemental mercury vapor, such as the cases of Mad Hatters disease that affected fur and felt hat makers (Asano et al., 2000). Methylmercury exposure is a more serious problem because the body absorbs ~95% of the methylmercury ingested through the gastrointestinal tract, lungs and skin, compared to 50-100% absorption of elemental mercury vapor inhaled through the lungs (Gochfeld, 2003; Honda et al., 2006). The ability for methylmercury to transfer to the fetus and cause permanent kidney damage and neurological disorders in humans (e.g., lack of muscle coordination and tremors) have led to increase awareness of the pollutant and monitoring of the mercury levels in the environment through the research community and government policies (Gochfeld, 2003; Honda et al., 2006).

1.2 Introduction to Source Identification Methods

To investigate the sources contributing to air pollutant concentrations at a receptor/sampling site, studies have used receptor models, such as Chemical Mass Balance (CMB) model (Davis et al., 1997; Heaton et al., 1992; Watson et al., 2001), Positive Matrix

Factorization (PMF) (Brinkman et al., 2006; Brown et al., 2007; Keeler, 2006; Lee et al., 2003), Unmix (Keeler, 2006; Lewis et al., 2003), and Factor Analysis/Principal Components Analysis (PCA) (Kim and Kim, 2001; Liu et al., 2007; Lynam and Keeler, 2006; Temme et al., 2007), as well as back trajectory modeling (Lee et al., 2003; Lee and Hopke, 2006; Lynam and Keeler, 2005), atmospheric pollutants ratio analysis (Jaffe et al., 2005; Lynam and Keeler, 2005; Manolopoulos et al., 2007b; Poissant et al., 2004), and correlation analysis (Han et al., 2004; Kim and Kim, 2001; Lindberg and Stratton, 1998; Lynam and Keeler, 2005). These models can identify the types of sources by using air pollutant concentrations measured at the source and/or sampling site, whereas dispersion models require prior knowledge of the source profiles and interactions between the pollutant and other chemical constituents, and meteorological forecast data to predict the air pollutant concentrations at the receptor (Hopke, 2003).

The CMB model has been used to identify sources of particulate matter and volatile organic compounds in air and pollutants in soil and deposition. Mathematically, each of the chemical species at the receptor is expressed as the sum of the products of the composition of chemical species at the source and the contribution of the source to the receptor (Hopke, 2003). The model assumption that all significant sources have been clearly identified and their emissions have been fully quantified (Capita, 1999; Chow and Watson, 2002) is invalid for identifying sources of Hg because there are potentially urban sources that have not been identified and reported in emission inventory. Therefore, this model was not chosen for the analysis of the Hg species data set. Positive Matrix Factorization (PMF) and Unmix models have been commonly used to apportion sources of particulate matter and pollutants in precipitation. One of the main advantages of the PMF and Unmix models over CMB models is that the number of sources and source profiles are not required to run the model. The models

only require the input of the measured pollutant concentrations at the receptor/sampling site. The models output a set of factors that contain some of the pollutants in the original data set, which can be used to characterize sources, and the relative impacts of each source to the pollutant concentrations at the sampling site (Eberly, 2005). Unlike the Unmix model, PMF has an additional feature that allows the input of data uncertainties, such as analytical and instrumentation uncertainties and detection limits (Keeler, 2006). Data containing large uncertainties would be down-weighted in the model due to low signal-to-noise ratio (Eberly, 2005), so that the more accurate data points would have a larger influence on the model. Principal Components Analysis (PCA) has been applied to atmospheric mercury concentrations to identify emission sources. Similar to the PMF model, PCA is used to group a large set of related variables (e.g., measured air pollutant concentrations) into a smaller set of factors while maximizing as much of the variance in the variables as possible (Garson, 2008; Pallant, 2005). One of the advantages of PCA is that there are several criteria that must be met to determine whether PCA is suitable for analyzing a data set and the number of factors to retain. The major disadvantage of statistical models, such as the PMF model and PCA, is the assumption that the Hg species do not undergo transformation during transport. Back trajectories track the movement of an air parcel from the sampling location backwards in time using meteorological data (Draxler and Rolph, 2003). Unlike PMF and PCA, the back trajectories model pollutant transport by wind. However, the trajectory path might not represent the path of an Hg plume due to plume dispersion. Atmospheric pollutants ratio analysis involves the comparison of air pollutant concentration ratios (e.g., NO_2/Hg, $PM_{2.5}$/Hg, SO_2/Hg, RGM/PHg) between the sources and receptor/sampling site. The advantage of ratio analysis over the PMF model and PCA is that it can identify sources based on the proximity of the sources to the sampling location, instead of

using factors, which may not be well defined to characterize the sources (Manolopoulos et al., 2007b). The potential disadvantages of this method are the uncertainties regarding emissions inventory data and the extent of the transformation processes (e.g., gas partitioning, chemical reactions) and deposition processes between a source and the sampling site (Jaffe et al., 2005; Manolopoulos et al., 2007b). Correlation analysis is useful for source identification because the correlation between Hg species and criteria air pollutants (e.g., NO_x, SO_2), which are commonly emitted from combustion or industrial sources, can be used to infer the types of sources. A more in-depth discussion and application of the models/data analysis methods are presented in the *Site Description and Data Analysis Methods* chapter.

1.3 Rationale and Significance of Research into Hg Source Identification

Mercury emitted from anthropogenic sources is capable of transporting in the atmosphere globally and transforming into inorganic forms, which can be readily converted into the toxic methylmercury compounds. Mercury speciation studies are, therefore, necessary because different physical and chemical properties of Hg species affect atmospheric transport, reactivity, bioavailability and toxicity of the chemical. Many of these studies are short-term, and the measurements of mercury species occurred in non-urban environments (Gabriel et al., 2005; Landis et al., 2004; Lynam and Keeler, 2005; Poissant et al., 2004; Poissant et al., 2005). There are several short-term (Gabriel et al., 2005; Kim and Kim, 2001; Lynam and Keeler, 2005) and long-term (Liu et al., 2007; Rutter et al., 2008; Stamenkovic et al., 2007) mercury speciation studies conducted in an urban atmosphere. The long-term Hg speciation measurements in urban environments are necessary because studies have found significantly higher Hg concentrations in urban atmosphere than background levels (background: 1.5-2.0 ng/m^3; urban atmosphere: 2.0-4.1 ng/m^3, Stamenkovic et al., 2007). The long-term studies conducted in Detroit (Liu et al., 2007)

and in Toronto (Song, 2005) observed large temporal variability and frequent concentration peaks of RGM and PHg<2.5 species over a period of one year, which were likely influenced by local and/or regional point sources. A recent analysis of total gaseous mercury (TGM) measured at the Canadian Atmospheric Mercury Measurement Network (CAMNet) sites over a 10-year period found that the changes to local and/or regional emission sources has led to a decline in TGM concentrations in rural areas and nearby urban centers (Temme et al., 2007). Mercury species concentrations measured in urban Detroit (Lynam and Keeler, 2005) and Milwaukee (Rutter et al., 2008) have been attributed to numerous point sources located within 100 km of the sampling site, such as coal utilities, steel mills and metals processing facilities, medical and municipal wastes facilities, and chemical manufacturing plants. The contribution of non-point sources to atmospheric Hg levels in urban atmosphere have not been studied extensively, but a recent study by Rutter et al. (2008) estimated that non-point sources in an urban area contributed ~67% of the measured GEM levels in Milwaukee. But the type of non-point sources within urban areas have not yet been identified and reported in emissions inventory. Lynam and Keeler's study (2006) inferred a portion of the Hg species levels measured in Detroit to vehicular emissions from nearby highways, which are also non-point sources. Natural surface emissions were reported to be affecting the TGM levels in Reno, Nevada because of the strong relationship between TGM, solar irradiance and temperature in the morning and between RGM and O_3 in the afternoon (Stamenkovic et al., 2007). RGM levels at night in Detroit have been attributed to the transport of oxidizing air masses from industrial areas and urban centers in Ohio (Lynam and Keeler, 2005), which led to the oxidation of GEM to RGM. These studies illustrate the significant long-term impacts of local and regional emission sources on atmospheric mercury levels and distributions in the urban atmosphere.

While much of the literature either focused on developing mercury emissions inventory or monitoring mercury levels in the environment, only recently have there been studies, such as those mentioned in the previous paragraph, to characterize and locate the types of sources contributing to the mercury levels at a particular sampling site. The study of urban areas is essential because higher Hg concentrations have been reported, but are the sources of Hg coming from local/regional point sources or from the urban area itself? Non-point, urban sources have not been identified in current emissions inventory due to limited research, but the presence of large human population and urban infrastructure could be adding to the global atmospheric mercury budget. In addition to source identification, some studies are attempting to quantify the proportion of mercury that each type of emission source contributes to the mercury levels measured at the sampling site. The results from source-receptor (or source apportionment) studies can be used to improve air quality models attempting to predict mercury levels downwind from known sources, and also have important engineering and environmental law and policy implications because of its potential to identify industries and/or companies in need of mercury emission controls and pollution prevention strategies. These measures are necessary to exceed the Canada-Wide Standards that were introduced to cap mercury emissions from base metal production, wastes incineration, and recently for coal-fired electric power generation facilities, which combine accounted for ~40% of the 12 tons of mercury emitted in the year 2000 in Canada (CCME, 2000).

1.4 Objectives of Study

The objectives of this study are to identify and locate the sources of atmospheric mercury in downtown Toronto based on the analysis of mercury speciation measurements, criteria air

pollutant data, meteorological data and Canadian emissions data between December 2003 and November 2004. This thesis focuses on the identification of mercury sources contributing to an urban atmosphere using Positive Matrix Factorization (PMF) model, Principal Components Analysis (PCA), Back Trajectory Modeling, Ratio Analysis, and Correlation Analysis. PMF, PCA and correlation analysis were applied to the entire data set between December 2003 and November 2004, whereas back trajectory modeling, ratio analysis and correlation analysis were used to identify sources that contributed to elevated Hg events.

2. Site Description and Data Analysis Methods

2.1 Location of Sampling Site and Sources of Hg

Mercury species concentrations were measured between December 2003 and November 2004 using an automated mercury speciation system (Tekran Inc., Toronto) that was situated on the rooftop of the Kerr Hall Building at Ryerson University (43° 39' 33.90"N, 79° 22' 45.60"W, see Figure 2.1). The Hg sampling site is located in the downtown Toronto, an urban centre with a population of 2.5 million (City of Toronto, 2006; Statistics Canada, 2006), and surrounded by a residential high-rise in the northwest direction and commercial and office buildings in the southwest direction. Stationary sources of Hg reported by the National Pollutant Release Inventory (NPRI) (Environment Canada, 2004c) include sewage treatment plants, metal production facilities, coal utilities, cement and concrete production facilities, and chemical manufacturing plants. Table 2.1 is a list of the top five mercury-emitting facilities in Ontario in 2004 based on emissions data from NPRI (Environment Canada, 2004c). The stationary sources within southern Ontario are located east of Toronto and in Whitby, Mississauga, Hamilton, Nanticoke, London, and Sarnia. Figure 2.1 is a map of Ontario and the locations of the Hg sampling site and various stationary sources of Hg.

Table 2.1: Major emission sources of mercury in Ontario in 2004

Top 5 Hg emission sources in Ontario

Source	Location	Hg emissions in 2004 (kg)
Coal utility	Nanticoke	134
Metals	Whitby	119
Metals	Hamilton	95
Coal utility	Courtright	46
Coal utility	Mississauga	46

Source: National Pollutant Release Inventory (Environment Canada, 2004c)

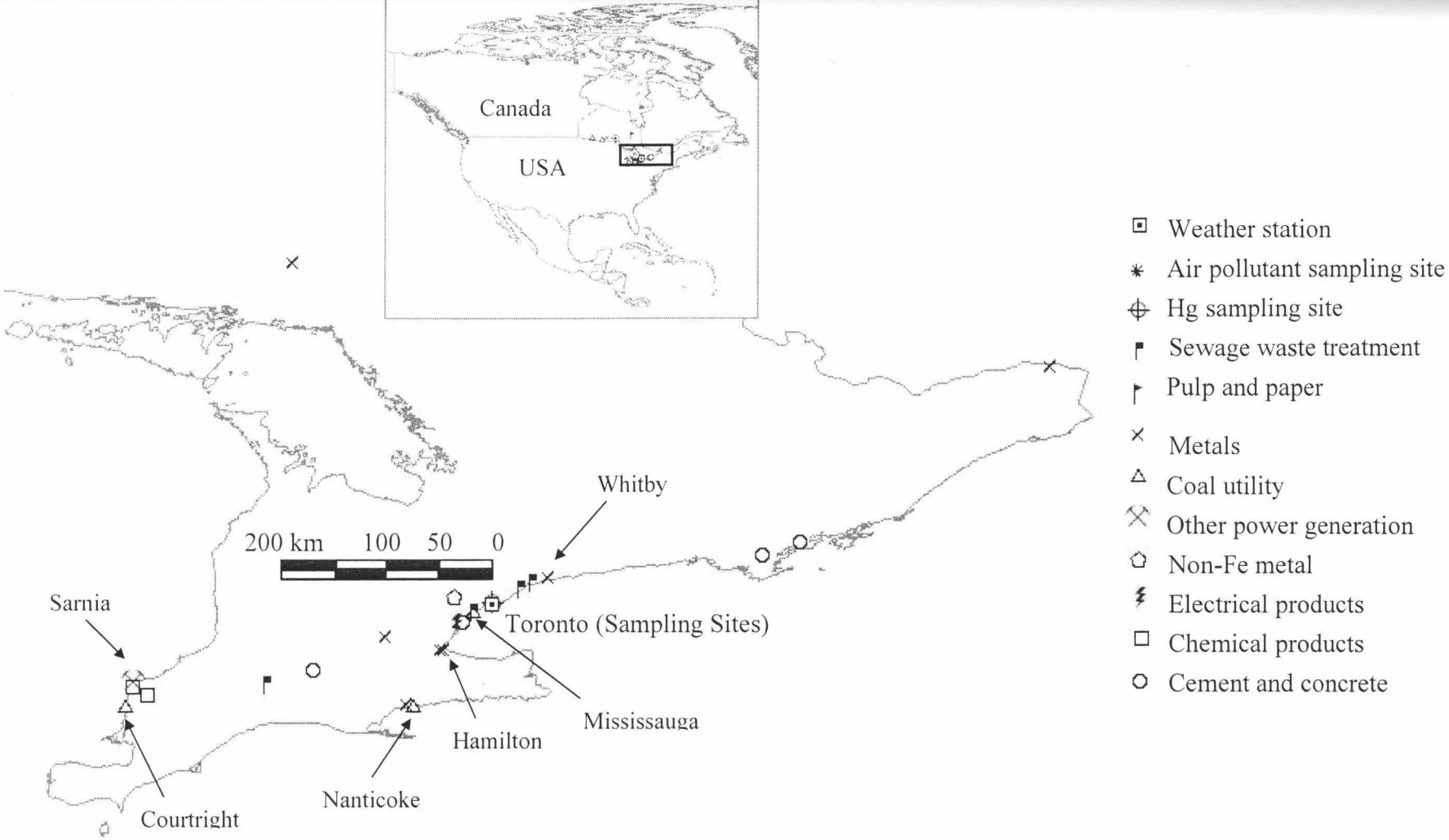

Figure 2.1: Location of Hg point sources in Ontario and Hg sampling site

2.2 Hg Speciation Data

Hg species concentrations were obtained from an Hg speciation study conducted in downtown Toronto (Master's Thesis by Xinjie Song, 2005). GEM (elemental Hg), PHg<2.5 (particulate Hg with an aerodynamic diameter less than 2.5 microns) and RGM (reactive gaseous Hg) concentrations were reported every other hour because of the 1-hour sampling and 1-hour desorption/analysis cycle. The GEM concentration in one hour was an average of the 12 GEM concentrations measured every 5 minutes in that hour. PHg<2.5 and RGM concentrations were calculated by summing the 4 PHg<2.5 concentrations and 3 RGM concentrations during the desorption hour.

2.3 Air Pollutants and Meteorological Data

Hourly CO, NO, NO_2, NO_x, $PM_{2.5}$, O_3, and SO_2 criteria air pollutant concentrations for the December 2003 to November 2004 period were obtained from the Ontario Ministry of the Environment's Air Quality website (2004). The air pollutant monitors, owned and operated by the Ontario MOE, are located approximately 1 km northwest of the Hg speciation system at a height of 10 m (43° 39'51"N, 79° 23'14"W). The weather station (WeatherHawk 232, USA) installed adjacent to the 1130 and 1135 models on the rooftop of Ryerson University recorded meteorological parameters, such as wind direction, wind speed, outdoor air temperature, relative humidity, solar radiation, rainfall and barometric pressure, every minute from May to December 2004. Hourly wind direction data from the Toronto Island Airport weather station (43° 37.8' N, 79° 24' W) installed at a height of 76.5 m was obtained from the Environment Canada's National Climate Data and Information Archive (2004b) website. The air pollutant concentrations and meteorological data corresponded to the end of the Hg sampling hour.

2.4 Detailed Model Description and Applications

This section describes in detail the models and data analysis methods used to interpret the December 2003 to November 2004 Hg species, air pollutants, meteorological, and emissions data sets. For each model/data analysis method, the data requirements, model parameters, and interpretation of the results in terms of source identification are discussed.

2.4.1 Positive Matrix Factorization (PMF) Model

Description of model: The PMF 1.1 model, which was developed by USEPA's Office of Research and Development (2007), calculates a specific pollutant concentration from P independent factors using the following mathematical expression (Eberly, 2005; Hopke, 2003):

$$x_{ij} = \sum_{k=1}^{P} g_{ik} f_{kj} \qquad \text{...Equation (1)}$$

where x_{ij} is the concentration of the jth specie at the receptor in the ith measurement; g_{ik} is the contribution of the kth factor on the ith measurement; f_{kj} is the mass concentration of the jth specie in the kth factor; P is the number of factors. The factors contain some of the measured pollutants, which are used to characterize the sources of mercury. Previous studies used chemical species (or trace elements) identified in the factors to determine the sources of particulate matter and pollutants in precipitation. Table 2.2 is a list of various types of sources and the major gaseous pollutants and/or trace elements emitted from the source.

Given the measured concentrations of each pollutant species, the PMF model estimates the values of g_{ik} and f_{kj} while trying to minimize the objective function, Q, which accounts for the uncertainties of the pollutant species.

$$Q = \sum_{i=1}^{n} \sum_{j=1}^{m} \left[\frac{x_{ij} - \sum_{k=1}^{P} g_{ik} f_{kj}}{s_{ij}} \right]^2 \qquad \text{...Equation (2)}$$

s_{ij} is the uncertainty of the jth specie on the ith measurement. In Equation (2), x_{ij} refers to the observed concentration of the jth specie, which is different from x_{ij} in Equation (1) that refers to the PMF model-predicted concentration of the jth specie. m and n denote the total number of pollutant species and total number of measurements, respectively.

Model inputs:

(1) An Excel spreadsheet file containing all the variables or in this analysis, non-missing Hg species and air pollutants concentrations. The model does not run if there is missing data (i.e., data that was not available). PHg<2.5 and RGM concentrations that were below the average detection limit of 4 pg/m^3 were not included in the model. The number of measurements that were missing or below detection limit was 566. The total number of concentrations for each pollutant that were inputted into the models was 3216.

(2) A separate Excel spreadsheet file containing uncertainty for each Hg species/air pollutant concentrations or a file containing the method detection limit and percent uncertainties for each pollutant. In the latter case, the method detection limit and percent uncertainties for each pollutant are used in an equation to determine the uncertainties of the concentrations.

Model parameters:

(1) **Signal-to-noise ratio.** After inputting the data files, the model displays a *Species Categorization* menu, which allows the analyst to down-weight or remove variables (e.g., air

pollutants) that have a small signal-to-noise ratio. The signal to noise ratio is dependent on the pollutant concentration relative to the uncertainties provided by the analyst. Down weighting reduces the variables influence on the model results. According to Paatero and Hopke (2003), a variable with a signal-to-noise ratio between 0.2 and 2 is defined as a "weak" variable and a variable with a ratio less than 0.2 is categorized as a "bad" variable. Weak variables are down-weighted in the model, while bad variables are removed. Based on these guidelines, none of the Hg species or air pollutants from the data set was down-weighted or removed.

(2) **Number of factors.** The number of factors, which ultimately represents the number of distinct sources, was varied during preliminary tests to assess the number of factors required to provide a good fit of the measured concentrations. This is determined by examining the R^2 value between the model-predicted and measured concentrations for each pollutant, which is displayed in one of the model's output files. The six-factor solution was selected in the final model. The number of factors that the user can enter ranges from 3 to 18. But the number of factors chosen should be less than the number of variables.

(3) **Number of random starting points.** The number of random starting points can be entered to determine which model-run will yield the lowest object function, Q, or the sum of least squares. Eight random starting points were chosen for the analysis. The PMF 1.1 model guide (Eberly, 2005) recommended at least five random starting points to ensure that the model achieves the lowest Q value. At eight random starting points, the Q values for each of the runs have reached a similar Q value, which is an indication that the lowest Q value has been achieved (Eberly, 2005). Increasing the number of random starting points would increase the model run time.

(4) **Random seed.** The analyst can choose to specify the seed used in random number generation or have randomly generated seeds. In the analysis, the randomly generated seed was selected. The random seed is the default setting, but the analyst could specify a seed so that another analyst can run the model in the exact same way using the same data set for the purpose of comparison. But if a seed were specified, the analyst would have to verify that other seeds would lead to the same model results.

Model outputs:

After running the model, the sum of least squares, Q, is shown for each of the eight random seeds. The random seed that minimizes the Q value was selected as the final model results. The PMF model outputs include:

(1) A file containing the factor profile or the chemical species concentrations for the factors (f_{kj} from Equation (1)), which are then used to characterize the source. The chemical species concentrations in the factors have the same units as the measured concentrations.

(2) A file containing the source contributions to the receptor concentrations (g_{ik} from Equation (1)) for every measurement. The source contributions provide information about the fraction each source is contributing to the measured Hg levels.

(3) A file containing the residuals or the difference between the model-predicted (x_{ij} from Equation (1)) and measured concentrations for each of the chemical species.

Model interpretation:

The chemical species concentrations for each factor were used to calculate NO_2/Hg, $PM_{2.5}$/Hg and SO_2/Hg. Hg refers to total mercury, which includes GEM, PHg<2.5 and RGM, in units of ng/m^3. NO_2 and SO_2 concentrations originally in units of parts per billion (ppb) were

converted to $\mu g/m^3$ using the Ideal Gas equation in order to keep the units of the ratios consistent (μg of pollutant/ng of Hg) (refer to sample calculations in the Appendix). Using emissions data from the National Pollutant Release Inventory, the NO_2/Hg, $PM_{2.5}$/Hg and SO_2/Hg for stationary sources in Ontario (emitting more than 10 kg of Hg in air in 2004) were determined. The emissions data have units of tons for criteria air pollutants (NO_2, $PM_{2.5}$, and SO_2) and kg for Hg emissions, so that the ratios of the source would be in units of tons of pollutant/kg of Hg. The range of the NO_2/Hg, $PM_{2.5}$/Hg and SO_2/Hg for the sources was compared with those calculated from the PMF model results to relate the factors to the Hg sources in Ontario. A potential issue of using the PMF model for gaseous pollutants is that there are an insufficient number of gaseous pollutants being measured to easily characterize the sources, unlike the large number of chemical species that can be measured from particulate matter or precipitation samples.

Although the factor profiles can identify the types of Hg sources that might be related to the measured Hg concentrations, it does not provide information about how much mercury each source is contributing to the measured Hg concentrations. To estimate the average Hg specie concentration from the kth factor, the product of the Hg specie concentrations of the kth factor and the source contributions (the product is equivalent to $f_{kj}\, g_{ik}$ from Equation (1)) are calculated and then averaged for the entire year (see sample calculations in the Appendix). Summing the model-predicted Hg specie concentrations from all the factors would yield the overall model-predicted Hg specie concentration, which is equivalent to Equation (1), $x_{ij} = \sum_{k=1}^{P} g_{ik} f_{kj}$. The average percent source contribution of Hg specie from the kth factor would be the average of the Hg specie concentration from the kth factor divided by x_{ij}. A high percent source contribution of Hg indicates that the source is strongly contributing to the Hg levels at the receptor site.

The PMF model can be evaluated by plotting the model-predicted concentrations against the measured concentrations and then obtaining the coefficient of determination, R^2, or by examining the residuals (the difference between model-predicted and measured concentrations).

Table 2.2: Chemical/trace element species used to characterize various types of emission sources

Source type	Major elements/pollutants emitted	References
Coal combustion	S, Se, NO_3^-	Keeler et al., 2006 citing Biegalski et al., 1998;
	Se is a source signature; also present are As, Fe, Co, Mn, Sb	Suarez and Ondov, 2002
	SO_2 is a primary emission with RGM for local coal-fired plants	Lynam and Keeler, 2006
	Elemental carbon, SO_4^{2-}, NO_3	
Oil combustion and incinerators	V, Ni	Keeler et al., 2006 citing Suarez and Ondov, 2002
	V, Co, Zn	Suarez and Ondov, 2002
Vehicle emissions	CO, NO_x (from NO and NO_2), hydrocarbons (e.g. aldehydes, ketones, carboxylic acids), PAN (peroxyacetylnitrate)	Twigg, 2007
	Elemental carbon, Ca, Ba (diesel emissions); high organic carbon/elemental carbon (gasoline emissions)[1]; Ca, Cu, Si, Ca (lubricating oil); Cu (metal brake wear), Si (heavy duty diesel emissions)	Lee and Hopke, 2006
	CO, NO_x, GEM	Lynam and Keeler, 2006
Iron/steel production	V, Cr, Mn, Fe	Keeler et al., 2006
	Al, Cu, Fe, Mn, Zn and carbon (metal processing/lead smelting); Fe, Mn, Cr (steel processing)	Lee and Hopke, 2006
	Cr, Fe, Mn	Suarez and Ondov, 2002
Municipal waste incineration	Zn, Pb, Cu, Cd	Keeler et al., 2006 citing Dvonch et al., 1999
Coke and lime production	Elemental carbon and several PAHs	Robinson et al., 2006
Cement kilns	Ca, Fe	Lee and Hopke, 2006 citing Chow et al., 2004
Paint pigment factory	Ba (paint pigment contains $BaSO_4$)	Lee and Hopke, 2006
Biomass burning	K, organic carbon, SO_4^{2-}	Lee and Hopke, 2006
Road salt	Na, Cl	Lee et al., 2003

[1] diesel-powered vehicles also produce high organic carbon/elemental carbon depending on operating conditions.

2.4.2 Principal Components Analysis (PCA)

Description of model: PCA is used to group a large set of related variables (e.g., measured air pollutant concentrations) into a smaller set of factors while maximizing as much of the variance in the variables as possible (Garson, 2008; Pallant, 2005). Similar to the PMF model, the factor consists of some of the measured air pollutants from the data set, which can be used to identify the types of sources. Unlike in the PMF model, PCA does not provide information about the percent contributions of each source to the receptor concentrations, or in other words, the impacts of the sources on the Hg concentrations at the sampling location. PCA also does not permit the data analyst to down-weight individual data points containing large uncertainties on the model. Large factor loadings (or correlation coefficients) between a factor and an air pollutant indicate that the pollutant is a major component of the factor. Table 2.2, which lists the major pollutants and trace chemical species emitted from various types of Hg sources, can be used to determine which source a factor may represent. PCA can be employed using statistical software, such as SPSS.

Model inputs:

(1) An Excel spreadsheet file containing all the variables (e.g., Hg species and air pollutants concentrations). PCA can be performed even if the data set contains missing data. However, to be consistent with the PMF model inputs, the data set without missing values and without PHg<2.5 and RGM concentrations below the average detection limit of 4 pg/m^3 was used in PCA. The total number of measurements for each pollutant that were inputted into the model was 3216.

Model parameters:

(1) **Factor Analysis Suitability:** To assess if the data set is suitable for PCA, SPSS performs the following statistical tests and the analyst decides whether factor analysis should be used for the data set. The first test is the Kaiser-Meyer-Olkin (KMO) measure of sampling adequacy. Tabachnick and Fidell (2001) suggested that a KMO value greater than 0.6 indicates a good factor analysis. The second test is the Bartlett's Test of Sphericity. The significance level of Bartlett's Test of Sphericity is $p<0.05$. In the analysis, the data set met both criteria.

(2) **Number of factors:** Kaiser's criterion, Scree Test and Parallel Analysis were used to determine which factors generated by the PCA model should be retained. According to Pallant (2005), Kaiser's criterion requires an eigenvalue > 1 to retain the factor. The number of factors to retain based on the Scree Test is determined by examining where the shape of the Scree plot changes to form an elbow (Pallant, 2005). The components on or before the bend are retained. Parallel Analysis generates average eigenvalues from randomly generated samples by specifying the number of variables and measurements. These average eigenvalues were generated from a computer software developed by Marley Watkins (2000). If the eigenvalue from PCA is larger than the eigenvalue generated from Parallel Analysis, then the factor is retained; otherwise, the factor is rejected (Pallant, 2005). The final PCA result was a four-factor model after carrying out the assessment. However, three-factor and five-factor solutions were also examined to assess whether these models could increase the percent variance of the data set explained and generate distinctively different factors.

(3) **Type of factor rotation:** The retained factors are then rotated using Varimax or Oblimin rotation techniques to interpret the results of the analysis. Varimax rotation was used in the

analysis because the sources are assumed to be independent. However, oblimin rotation was also attempted to verify that the factors/components are not strongly correlated with each other.

Model outputs:

(1) A table illustrating the percent variance of the data explained by each of the four rotated components.

(2) A table illustrating the factor/component loadings, which are the correlation coefficients between the variables in the data set and the factors/components extracted. The component loadings will be used to characterize the sources. The factor loadings can be positive or negative, unlike the PMF model that limits the solution to non-negative values (Eberly, 2005). This is relevant to source identification because normally we are interested in a positive relationship between the factor and variables (e.g., Hg species and/or air pollutants).

Model interpretation:

By examining the loadings on each of the variables in each factor/component, the sources can be identified. A factor with strong GEM and NO_2 or NO_x loadings indicate combustion sources, such as vehicle combustion and/or industrial processes (Lynam and Keeler, 2006). Coal combustion is likely a factor if there are strong RGM and SO_2 loadings (Lynam and Keeler, 2006). RGM and O_3 loadings are indicative of photochemical processes converting GEM to RGM (Kim and Kim, 2001; Lynam and Keeler, 2005, 2006).

The percent variance of the data explained by each factor is reported to evaluate how well the model represents the measured Hg data set. The percent variance explained by each factor is calculated by summing the factor loadings of all the air pollutants and then dividing by the

number of air pollutants used in PCA. A high percent variance explained by a factor suggests that it represents the Hg data set well.

2.4.3 Back Trajectory Modeling

Description of model: The PMF and PCA models discussed so far require only the observed measurements and emissions data to identify the types of sources affecting the receptor site. These statistical models have not incorporated the effects of meteorological conditions on the transport of air pollutants from the source to receptor. Trajectory models use meteorological data that has been generated from other models, which use data obtained from weather monitoring stations on land and water, rawinsonde (device used in weather balloons to measure wind direction and speed), wind profilers, and satellites (Gebhart, 2005). The 3 to 4 dimension meteorological data is spatially interpolated onto a model grid and provided at regular time intervals before being inputted into trajectory models. To investigate whether the meteorological conditions during elevated GEM events favored the transport of Hg from the regional sources to the sampling site in Toronto, 48-hour back trajectories corresponding to the period of the elevated Hg events were generated using the NOAA Air Resources Laboratory web-based HYSPLIT (HYbrid Single-Particle Lagrangian Integrated Trajectory) model (Draxler and Rolph, 2003; Rolph, 2003). The HYSPLIT model simulates that transport of an air parcel by wind and estimates the position of the parcel using velocity vectors that have been spatially and temporally interpolated onto a grid (Draxler and Rolph, 2003; Rolph, 2003). The trajectory represents the path of a single particle from the time of its initial release and does not account for particle dispersion (Draxler and Rolph, 2003; Rolph, 2003). Back trajectory modeling was applied to

only the elevated Hg events (GEM concentration > 20 ng/m^3). There were a total of eight elevated Hg events throughout the entire monitoring campaign.

Model inputs:

(1) **Meteorological Data:** The EDAS (Eta Data Assimilation System) archived meteorological data, developed by the National Weather Service's National Centers for Environmental Prediction (NCEP), were selected as the meteorological input to the model. The meteorological data has been interpolated onto a 40 km grid that spans the United States and Canada. The vertical resolution covers 26 pressure surfaces from 1000 hPa (mbar) to 50 hPa. The meteorological data is provided every 3 hours. The EDAS 40 km meteorological data was chosen because it was the highest spatial resolution data set available on the web version of HYSPLIT.

(2) **Trajectory starting location:** The latitude and longitude coordinates of the Hg sampling site were entered, i.e. 43° 39' 33.90"N, 79° 22' 45.60"W, to represent the starting location of the trajectory.

(3) **Date of archived meteorological data:** The archived meteorological data was stored as 15-day files. Each month contains two data files: one for the first half of the month and the other for the second half. The data file was selected based on the date of the elevated GEM event.

Model parameters:

(1) **Trajectory direction:** Either forward or backward trajectories can be selected. For source identification studies, backward trajectories were chosen.

(2) **Vertical motion:** The model allows the choice of model vertical velocity, isobaric (trajectory follows a constant pressure surface) or isentropic (trajectory follows a constant potential temperature surface) to calculate vertical motion. Model vertical velocity means that the model's vertical velocity fields are used in the calculation and was recommended for most applications.

(3) **Start time:** The time in UTC (universal time, coordinated) corresponding to the end of the elevated GEM episode was entered. The HYSPLIT model provides a table to convert between Eastern Standard Time and UTC.

(4) **Total run time:** This is the time duration of the trajectory. 48-hour trajectories were selected for all the elevated GEM episodes.

(5) **Trajectory starting heights:** Trajectory starting heights of 15 m, 50 m and 500 m were chosen to represent the height of the sampling inlet, buildings in the downtown core, and above the urban structure canopy, respectively. Trajectories were generated at three different heights because the model is sensitive to starting heights, which can yield very different trajectory paths (Gebhart et al., 2005).

Model outputs:

(1) GIS shapefile (a file format used specifically in Geographic Information Systems software) that can be imported into ArcView GIS software to plot maps illustrating the sources, Hg sampling site, and back trajectories corresponding to each elevated GEM event.

Model interpretation:

The trajectory paths indicate whether an air parcel had passed through sources that emit Hg during the elevated GEM episodes. The model provides information about the types and location of the Hg sources contributing to the elevated GEM concentrations at the receptor site.

One of the important considerations in using back trajectory modeling is that the resolution of the meteorological data should reflect the scale of the study, e.g., global, national, regional, local and/or urban scale, because a large portion of the model uncertainties have been attributed to the input meteorological data (Gebhart et al., 2005; Schichtel and Wishinski, 1996). Back trajectories might not reflect the observed meteorological conditions because of the spatial and temporal interpolation of the meteorological parameters (Draxler and Rolph, 2003; Rolph, 2003). Recent modeling studies conducted over urban areas found that finer resolution meteorological data is necessary to simulate pollutant transport in an urban atmosphere and resolve local sources (Arain et al., 2007). However, the task of generating higher resolution data is currently technically and computationally demanding (Stein et al., 2007; Dr. L. Zhang, 2007, personal communication).

2.4.4 Ratio Analysis

Description of analysis: Ratio analysis is a comparison of the NO_2/Hg, $PM_{2.5}$/Hg and SO_2/Hg between Hg sources and those measured at the sampling location to identify the types of sources affecting a receptor site. RGM/PHg<2.5 and wind direction data during elevated Hg events have also been analyzed to assess whether regional sources could be affecting the Hg levels at the sampling location, since a decreasing RGM/PHg<2.5 indicates an aging mercury plume. Previously, NO_2/Hg, $PM_{2.5}$/Hg and SO_2/Hg were used in the PMF model results to relate the factors and sources.

Data required:

(1) Hg species and air pollutant concentrations during the elevated GEM events (GEM concentration > 20 ng/m^3). NO_2 and SO_2 concentrations in units of parts per billion (ppb) were

converted to $\mu g/m^3$ using the Ideal Gas equation at standard temperature and pressure (refer to sample calculations in the Appendix). The unit conversions were necessary because the units of the NO_2/Hg, $PM_{2.5}$/Hg and SO_2/Hg at the sampling site must be µg of air pollutant/ng of total Hg in order to compare with the source ratios, which will be in units of tons of air pollutants/kg of total Hg. Total Hg concentration is the summation of elemental Hg (GEM), particulate Hg (PHg<2.5) and reactive gaseous Hg (RGM) concentrations.

(2) Wind direction data measured at Ryerson University and Toronto Island Airport corresponding to the time of the elevated GEM events. Wind directions observed at Ryerson University would likely be affected by buildings and commercial area located south/southwest of the sampling site. Thus, the wind direction data from the Toronto Island Airport station (located south/southwest of the sampling site in Lake Ontario) can be used to confirm the southwest trajectory paths generated from the HYSPLIT model.

(3) 2004 emissions data (Hg, NO_2, $PM_{2.5}$, and SO_2) from stationary Hg sources in Ontario. In the NPRI, Hg emissions into the atmosphere were reported in kilograms, while NO_2, $PM_{2.5}$, and SO_2 emissions were reported in tons.

Interpretation of results:

Similar NO_2/Hg, $PM_{2.5}$/Hg and SO_2/Hg between a source and those measured at the sampling location indicate that the source is affecting the sampling site. Sources with atmospheric pollutant ratios much larger than the receptor/sampling site are unlikely to be contributing to the sampling site because of the large amount of deposition that would have to occur (Manolopoulos et al., 2007b). Decreasing RGM/PHg<2.5 (indicates gas partitioning processes) from a constant

wind direction suggests that a regional source located in that wind direction is potentially contributing to the Hg levels at the sampling site (Lynam and Keeler, 2005).

2.4.5 Correlation Analysis

Description of analysis: Correlation analysis is often performed on a set of variables to determine the strength of the relationship between two observed variables and whether the relationship is positive or negative. This is useful for source identification because the correlation between Hg species and criteria air pollutants, which are commonly emitted from combustion or industrial sources, can be used to infer types of sources. Recent literature and atmospheric Hg models have used correlation analysis between Hg species and NO_x, O_3 and SO_2 as a method to identify sources of RGM (reactive gaseous mercury) (Han et al., 2004; Kim and Kim, 2001; Lynam and Keeler, 2005). RGM can be emitted into the atmosphere directly as well as indirectly through the oxidation of GEM (elemental mercury) by oxidants, such as O_3, halogens, and hydroxyl radicals in the atmosphere (Lindberg and Stratton, 1998). Correlation analysis will be conducted using statistical software, such as SPSS. Pearson r correlation analysis with a significance level of $p<0.05$ was chosen.

Data required:

(1) Hg species and air pollutants concentrations segregated into winter, spring, summer, and fall. The seasonal analysis was necessary because ozone levels are also affected by meteorological parameters, such as solar radiation and temperature (Kim and Kim, 2001).

(2) Hg species and air pollutants concentrations corresponding to the time of the eight elevated GEM episodes (GEM concentration > 20 ng/m^3).

Interpretation of results:

Correlations between Hg, CO and NO_x have been used to relate mercury levels at the sampling site to industrial or vehicular combustion sources (Lynam and Keeler, 2006); RGM-SO_2 correlations have been used to identify coal combustion (Han et al., 2004), and RGM-O_3 correlations have been examined to identify the photochemical reactions converting GEM to RGM (Han et al., 2004; Lindberg and Stratton, 1998; Lynam and Keeler, 2005; Sillman et al., 2007). Positive correlations between model-predicted GEM and RGM indicate direct emissions of RGM, whereas anti-correlations indicate that RGM is indirectly produced from the oxidation of GEM (Sillman et al., 2007).

2.5 Summary of Models/Data Analysis Methods

Table 2.3: Summary of the models/data analysis methods used in this study, the data requirements and model parameters, and model interpretation

	Statistical models	Ratio Analysis	Trajectory model
Types	▪ Positive Matrix Factorization 1.1 model (PMF) ▪ Principal Components Analysis (PCA) ▪ Correlation Analysis (CA)	▪ Air pollutants to Hg ratios (NO_2/Hg, $PM_{2.5}$/Hg, SO_2/Hg) ▪ RGM/PHg<2.5	▪ HYSPLIT back trajectory model (web version)
Required data/model parameters	▪ Hg species and air pollutant data (entire data set) ▪ Elevated GEM data ▪ Data uncertainties (for PMF model) ▪ NPRI emissions data of Hg sources in Ontario	▪ Elevated GEM data ▪ NPRI emissions data of Hg sources in Ontario ▪ Wind direction data	▪ Elevated GEM data ▪ EDAS 40km archived meteorological data ▪ 3 trajectory starting heights ▪ Duration: 48 hrs ▪ Map showing location of emission sources
Model interpretation	▪ Identifies sources from factor profiles (PMF) and factor loadings (PCA) ▪ Contributions of sources to receptor measurements (PMF) ▪ Identifies RGM sources due to direct emissions and/or photochemical processes (CA)	▪ Identifies types of sources (e.g., chemical production, metal production, coal utilities, cement production, or sewage treatment) and whether Hg plumes came from regional sources	▪ Identifies sources that trajectories passed through

3. Results and Discussion

3.1 PMF Model Results

The PMF model results, shown in Table 3.1, illustrated that factors 4, 5 and 6 contribute to most of the Hg measured at the sampling site, and factors 1, 2 and 3 combined contribute to less than 12% of the measured GEM, PHg<2.5 or RGM concentrations. Using the factor profiles and emissions data in 2004 from the National Pollutant Release Inventory (NPRI) (Environment Canada, 2004c), air pollutant to Hg ratios (e.g., NO_2/Hg, $PM_{2.5}$/Hg and SO_2/Hg) were calculated for the model factors and sources (see Tables 3.1 and 3.2). The Hg in the ratios refers to the sum of the atmospheric mercury species. The NPRI only reports criteria air pollutant emissions for stationary sources, and our analysis have focused only on those sources in Ontario that emitted more than 10 kg of Hg in 2004. Air pollutants to Hg ratios for the model factors that are within the range of the source ratios indicate that the factor and source are related. The following section describes what each of the factors could represent.

Based on the factor profiles in Table 3.1, factor 4 is likely related to industrial sources and photochemical processes because the profile contains some nitrogen oxides and sulfur dioxide and large amounts of ozone. Sunlight breaks down nitrogen dioxide into nitrogen oxide and a free oxygen atom, which can react with oxygen to form tropospheric ozone. The emission of other air pollutants, such as volatile organic compounds, could prevent the natural destruction of tropospheric ozone resulting in a build up of ozone. Factor 4 might be associated with industrial sources, such as chemical products manufacturing and primary metal production, because of the similar NO_2/Hg and SO_2/Hg ratios between the factor and sources (see Table 3.1 and 3.2). However, there is large variation in the air pollutants to Hg ratios for primary metal production facilities in Ontario, and the nearest facility is located 50-60 km from the sampling

site (e.g., in Whitby or Hamilton – see Figure 2.1). The closest chemical manufacturing plant is about 300 km from the sampling site (e.g., in Sarnia) and not a major emitter of Hg (see Table 2.1), but the use of chemical-manufactured products in an urban city is potentially a source of Hg (Hagreen and Lourie, 2004). Factor 4 contributes 4.3% GEM, 0.8% PHg<2.5 and 10.9% RGM.

Table 3.1: Factor profiles (f_{kj} from Eqn.(1)), ratio of air pollutants to Hg (µg of pollutant/ng of Hg), and percent Hg source contributions to the measured Hg concentrations generated by the PMF model

	Factor 1	Factor 2	Factor 3	Factor 4	Factor 5	Factor 6
Mass concentrations						
GEM (ng/m^3)	0.19	0.35	0.01	0.20	3.90	1.3×10^{-3}
PHg<2.5 (pg/m^3)	0.17				4.84	18.64
RGM (pg/m^3)		0.23	1.27	1.63	3.61	8.24
NO (ppb)	7.29	0.13	0.04	0.23	0.06	
NO_2 (ppb)	1.77	16.18	0.04	0.98	0.69	0.48
NO_x (ppb)	9.14	16.54	1.1×10^{-3}	1.32	0.77	0.47
O_3 (ppb)	0.08	0.23		22.63	0.50	
$PM_{2.5}$ (µg/m^3)	0.01		7.20		0.18	
SO_2 (ppb)	0.04	0.84	0.57	0.44		0.30
Ratio of air pollutants to Hg						
NO_2/Hg	19	96	9	10	0.36	35
$PM_{2.5}$/Hg	0.060		850		0.047	
SO_2/Hg	1	7	192	6		30
% source contributions						
GEM	4.1	7.5	0.2	4.3	84.0	0
PHg<2.5	0.7	0	0	0.8	20.3	78.1
RGM	0	1.5	8.5	10.9	24.1	55.0
Potential sources (from comparison of ratios in table 3.1 and 3.2)	Metals production	Metals production	Cannot be identified from inventory	Metals production, chemical production, ozone photochemical processes	Sewage treatment	Metals production, chemical production

Table 3.2: Range of air pollutant to Hg ratios for stationary sources (tons of pollutant/kg of Hg) in 2004 in Ontario. Source of air emissions data: National Pollutants Release Inventory (Environment Canada, 2004c).

	Cement & concrete	Chemical products	Fossil fuel power generation	Metal/steel production	Sewage treatment
NO_2/Hg	55-562	3-44	54-180	1-135	0.6-4
$PM_{2.5}$/Hg	4-29	0.2-9	0.3-15	0.2-254	0.04-0.1
SO_2/Hg	57-541	7-465	136-563	0.1-20327	0.2-0.9
# of facilities*	5	2	5	7	4

* facilities that emitted more than 10 kg of Hg in 2004

Factor 5 has a profile with a high GEM concentration, but relatively low PHg<2.5, RGM and other criteria air pollutant concentrations. Hence, the NO_2/Hg and $PM_{2.5}$/Hg ratios for factor 5 are very small and are comparable to the ratios found in sewage treatment facilities, which are located 20-30 km from the sampling site (e.g., in Toronto east, Pickering, Mississauga). This factor contributes 84.0% GEM, 20.3% PHg<2.5 and 24.1% RGM. Factor 6 contains PHg<2.5, RGM and trace amounts of nitrogen oxides and sulfur dioxide, and contributes to most of the PHg<2.5 and RGM, 78.1% and 55.0%, respectively. The NO_2/Hg and SO_2/Hg ratios of factor 6 are within the range of the ratios for chemical products and primary metal production sources. This is similar to factor 4, but without the influence of photochemical processes involving ozone. Factors 1 and 2, which have minor contributions to the measured Hg levels, might belong to primary metal production as well based on similar NO_2/Hg and SO_2/Hg ratios between the factors and sources. Factor 3 does not appear to be associated with the stationary sources in Ontario because of the relatively large $PM_{2.5}$/Hg ratio. Our analysis found that cement and concrete production and fossil fuel power generation (i.e., coal combustion) were likely not

contributing to the Hg species concentrations in Toronto, since both the NO_2/Hg and SO_2/Hg were outside the range of the ratios of these sources.

As shown in Table 3.1, sewage treatment contributed ~84% of the GEM levels, while metals and chemical production contributed ~16% of the GEM levels. Sewage treatment contributed ~20% of the PHg<2.5 levels, and metals and chemical production contributed ~80% of the PHg<2.5 levels. Sewage treatment contributed ~24% of the RGM levels, and metals and chemical production contributed ~76% of the RGM levels.

3.1.1 Evaluation of PMF Model

The model-predicted Hg species concentrations from all factors, calculated using the PMF model equation (Equation (1)) discussed in section 2.4.1, provided a good fit of the measured concentrations of GEM and PHg<2.5 as evident by the large R^2 values shown in Figure 3.1 (a) and (b). The R^2 values were 1 and 0.97, respectively. However, the PMF model only provided a moderate fit of the measured RGM concentrations, since the R^2 value was 0.45 (see Figure 3.1(c)). This might because the PMF model does not attempt to over fit the extreme data points and assumes that the chemical species do not undergo transformation between the source and receptor site. During preliminary model test runs, the number of factors was varied to achieve a larger R^2 value for the three Hg species. There was a significant improvement in the coefficient of determination when the number of factors was increased from 4 to 6, but insignificant improvements from a 6 to 7-factor solution. The plot of the residuals for GEM, PHg<2.5 and RGM (see Figure 3.1 (d) – (f)) illustrate that the model fits were acceptable. The residuals plot appeared random for all three Hg species, and only 0.75%, 0.12% and 1.52% of the predicted GEM, PHg<2.5 and RGM concentrations were beyond three times the standard deviation of the residuals.

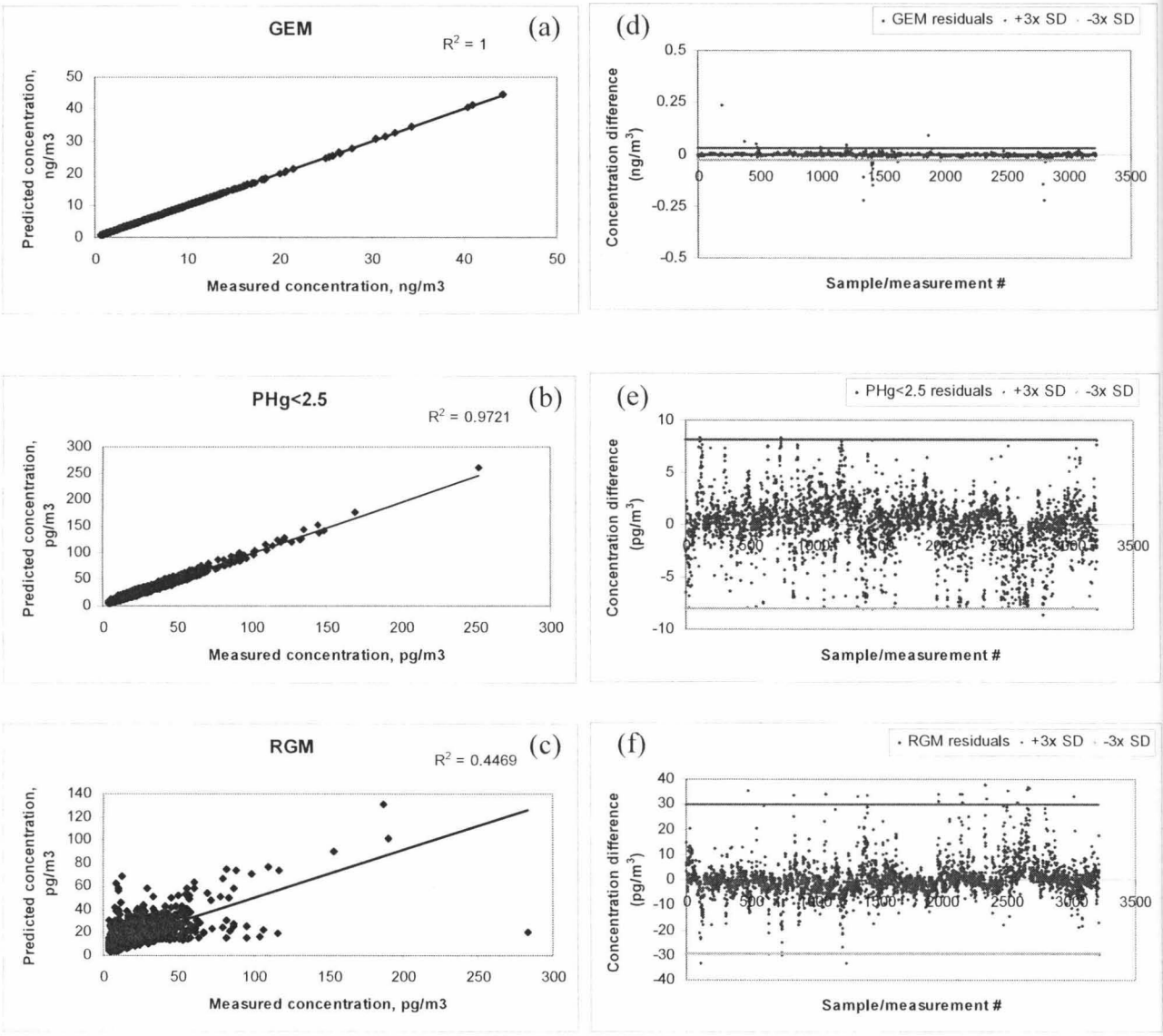

Figure 3.1: PMF model predicted concentrations versus measured concentrations for (a) GEM, (b) PHg<2.5, and (c) RGM, and Residual (PMF predicted concentration – measured concentration) distribution for (d) GEM, (e) PHg<2.5, and (f) RGM. 3x SD = three times the standard deviation of the residuals.

3.1.2 PMF Model Results from Literature

The PMF model was used in many studies for identifying and quantifying the sources that contributed to particulate matter and wet deposition in the environment. $PM_{2.5}$ measured in St. Louis, Missouri was affected by local point sources, such as zinc smelting, copper production, steel mills and lead smelting (Lee and Hopke, 2006), which contributed 16-18% of the $PM_{2.5}$. Regional sources located in Ohio, Iowa and Kansas that contained secondary sulfate and nitrate contributed 51-60% of the measured $PM_{2.5}$, and vehicular emissions contributed 17-26% of the measured $PM_{2.5}$. Long-range transport of dust from Africa also contributed to 3% of the measured $PM_{2.5}$. The study by Lee and Hopke (2006) analyzed 26 elements in the particulate matter samples and thus, was able to generate distinct factor profiles that can better characterize the types of sources. The PMF model was able to explain about 90% of the variance in the measured $PM_{2.5}$ data. The study by Keeler et al. (2006) used PMF to apportion sources of Hg wet deposition in Steubenville, Ohio. The site was surrounded by 17 coal-fired utility boilers within a 100 km radius of the sampling site. Six sources were identified, which included iron/steel production, oil and incineration, crustal, coal combustion, phosphorous and molybdenum. Not surprisingly, coal combustion contributed 73% of the Hg wet deposition at the sampling site, while 6% and 2% were apportioned to iron/steel production and phosphorus emitting sources. The coefficient of determination was 0.85 for the model predicted Hg concentrations versus measured Hg concentrations in wet deposition. The study by Lee et al. (2003) is the most relevant to the current analysis because the sampling site was also located in downtown Toronto. Using the PMF model, the study apportioned most of the $PM_{2.5}$ to four major sources. The source contributions were 26% for coal combustion and secondary sulfate, 36% for secondary nitrate (from power plants and transportation), 15% for secondary organic

aerosols (from biomass burning in the US), and 10% for vehicle emissions. The model identified other factors that might be related to sources, such as road salt, coal/oil combustion, industrial (e.g., steel production, mining, metal processing, smelters and incineration), and construction, but source contributions were smaller. The PMF model was able to explain 97% of the variance in the measured $PM_{2.5}$ data in Toronto. The studies in St. Louis, Steubenville, and Toronto apportioned particulate matter to local coal combustion and industrial sources, whereas the PMF model did not apportioned Hg in Toronto to coal combustion. The PMF model results from this study and Lee et al. (2003) are different because of the different pollutants being studied and different chemical species that were used to characterize the coal combustion factor. The coal combustion factor in the study by Lee et al. (2003) consisted of secondary pollutants, such as sulfate (SO_4^{2-}), ammonium (NH_4^+) and phosphate (PO_4^{3-}), and selenium (Se), which is an element also commonly found in metal ores, whereas SO_2 was used to characterize coal combustion in this study.

3.2 PCA Results

The correlation coefficients or factor loadings between the air pollutants and each factor are tabulated in Table 3.3. Four unique factors were extracted from PCA. The factors generated from PCA contain some of the variables in the data set and are used to characterize the sources, similar to the PMF model factors. Air pollutants that are strongly related to the factor have large correlation coefficients (i.e. greater than 0.50). PCA results indicated that the Hg species have a moderate to weak relationship with factors 1, 3 and 4 and a strong relationship with factor 2. Based on the factor loadings in Table 3.3, factor 1 might be related to combustion sources, such as vehicles and/or industrial processes, because of the high factor loadings for the nitrogen

oxides species (NO, NO_2 and NO_x). Factor 2 contains high factor loadings for Hg species, but no factor loadings for the criteria air pollutants except for $PM_{2.5}$. Thus, factor 2 is not well defined and also might not be related to combustion sources.

Table 3.3: PCA factor loadings and percent variance of the data explained by each factor

	Factor 1	Factor 2	Factor 3	Factor 4	
GEM	0.19	0.80	-0.16		
PHg<2.5		0.85			
RGM		0.75	0.27	0.16	
NO	0.88		0.11		
NO_2	0.85			0.24	
NO_x	0.98				
O_3	-0.68		0.62		
$PM_{2.5}$	0.27	0.12	0.84	0.19	
SO_2	0.13		0.15	0.96	
Overall R^2 (% variance explained)	33.7	21.5	13.5	11.6	80.3

Factor 3 has a weak, negative factor loading for GEM and a moderate, positive factor loading for RGM. This factor is also strongly related to O_3 and $PM_{2.5}$ and weakly related to NO and SO_2. This suggests that factor 3 is associated with photochemical and combustion processes. Photochemical processes and combustion are related because the byproducts from combustion can lead to the formation of secondary pollutants, such as O_3. O_3 can oxidize GEM to form RGM, which might explain the negative and positive factor loadings for these two species. Factor 4 is also representative of many types of combustion sources (e.g., from vehicles, industrial processes, fossil fuels, etc.) because it contains weak factor loadings for RGM, NO_2 and $PM_{2.5}$ and strong loadings for SO_2.

Comparison of the factor descriptions from PCA with the emissions data reported by facilities suggests that industrial processes from chemical product manufacturing and sewage treatment, and combustion processes from primary metals production are likely affecting the Hg levels in Toronto. Vehicular combustion is also a potential source of Hg mainly because of the presence of nitrogen oxides in vehicular exhaust and the close proximity of the sampling site to roads and highways in downtown Toronto. As previously discussed, the factor profiles are not unique enough to differentiate between the different types of combustion processes. The factor loadings for RGM and SO_2 in this study do not agree with those identified as coal combustion in the studies by Liu et al. (2007) and Lynam and Keeler (2006). In these studies, the coal combustion factor loadings for RGM and SO_2 were 0.79-0.86 and 0.72-0.73, respectively. Thus, coal combustion is likely not a source of Hg in Toronto. This finding is also consistent with PMF model results.

The description of factor 2 from PCA is not related to any of the Hg sources reported on NPRI, but factor 2 does represent a significant source because it explains ~22% of the variance in the data set and has high factor loadings for all the Hg species. Further investigation into this source is required. However, we speculate that the unidentified Hg source might be related to non-point, urban sources (e.g., Street pavement dust, roofs, windows and soils has been reported by Eckley and Branfireun (2008) as sources of Hg emissions in Toronto and Austin, Texas; Hagreen and Lourie (2004) estimated that fluorescent lamps and thermometers commonly found in buildings directly release ~1,100 kg of Hg/year in Canada; fugitive (non-duct/stack) Hg emissions from a Hg cell chlor-alkali building, estimated at ~500 g of Hg/day, have also been reported by Southworth et al. (2004)) because Hg concentrations in urban airshed are typically higher than those in rural airshed, and the Toronto site is not closely surrounded by major point

sources as shown in Figure 2.1. Within 100-km of the sampling site in Toronto, the major point sources (i.e. top 5 emitters of Hg in Ontario) include two metals production plants located in Whitby and Hamilton (~60 km away) and the Lakeview power plant located in Mississauga (~17 km away), which was still in operation in 2004. The number of major point sources within 100-km of the sampling site in Toronto is significantly less than those within the same distance from the sampling sites in Detroit, Steubenville, and Milwaukee. The Detroit site was affected by 6 coal utilities, 4 medical wastes, 4 municipal wastes, 13 steel, and 1 other metals facility within 30-km of the sampling site (Lynam and Keeler, 2005). The Steubenville, Ohio site was surrounded by 17 coal-fired utilities within 100-km of the sampling site (Keeler et al., 2006). The Milwaukee, Wisconsin site was enclosed by 5 coal utilities, 1 steel mill/blast furnace, and 1 chemical manufacturing plant within 100-km of the sampling site (Rutter et al., 2008).

3.2.1 Evaluation of PCA

The factors generated from PCA are suppose to be representative of the Hg species and criteria air pollutants data set, and they are evaluated using percent variance explained or the overall factor R^2. The percent variance explained for each factor (see Table 3.3) is calculated by summing the factor loadings of all the air pollutants for each factor and then dividing by the number of air pollutants used in PCA. The total percent variance explained by the four factors is about 80%. About 54% of the variance of the measured data is attributed to combustion processes, ~14% of the variance is explained by a factor related to both combustion and photochemical processes involving ozone, while ~22% is associated with source(s) that lacks a source profile.

3.2.2 PCA Results from Literature

Principal Components Analysis (PCA) has been used for developing source-receptor relationships for Hg. Factor analysis was applied to total gaseous mercury (TGM) concentrations (i.e., sum of GEM and RGM concentrations), other air pollutants and meteorological variables that were measured in Seoul, Korea (Kim and Kim, 2001). PCA results on the fall daytime data set generated two factors. The first factor, which explained 57% of the variance in the data, contained Hg and criteria air pollutants (CH_4, CO, NO_x and SO_2), and the second factor, which explained 16% of the variance in the data, consisted of Hg, temperature, relative humidity and ozone. Unlike the fall daytime data set, the fall nighttime and summer daytime and nighttime data sets each generated a factor composed of criteria air pollutants that explained 40-57% of the variance in the data set, and two other factors containing meteorological variables. The data analysis indicated that the factors affecting daytime Hg levels are different between summer and fall. The study of potential sources affecting the Hg species levels and distribution during four separate sampling campaigns (July and September 2000, July 2001, July 2002) in Detroit was also conducted using PCA (Lynam and Keeler, 2006). Lynam and Keeler (2006) found that GEM was associated with a factor containing CO and NO_x likely emitted from vehicles on nearby highways. This factor explained 17% of the variance in the data set. RGM was linked to a photochemistry factor due to high factor loadings for RGM and O_3 and a coal combustion factor, which had high factor loadings for both RGM and SO_2. The coal combustion factor was expected because several coal-fired facilities were located near the sampling site. The percent variance explained was 33% for the photochemistry factor and 25% for the coal combustion factor. PCA was performed on the annual Hg species concentrations measured in 2003 at the same sampling location by Liu et al. (2007). The factors identified in the study by

Liu et al. (2007) were related to photochemical processes involving O_3, local coal combustion sources and transport of polluted regional air masses, and seasonal meteorological conditions. The data analysis of TGM collected from 11 CAMNet (Canadian Atmospheric Mercury Measurement Network) sites over a 10-year period (1995-2005) was characterized by PCA (Temme et al., 2007). Using PCA, Temme et al. (2007) identified two factors that combined explained 50% of the variance in the data set. These factors were related to seasonal variability in TGM concentrations (e.g. higher TGM concentrations in the winter and spring compared to summer and fall at most CAMNet sites) and changes to local natural or anthropogenic sources that have led to significant decreases in TGM concentrations in certain rural CAMNet sites.

3.3 Data Limitations

The NPRI was useful for identifying the types of stationary sources that were impacting the Hg concentrations at the sampling site; however, it did not include the potential impacts that mobile sources, such as vehicles, can have on Hg levels in the urban environment. This is relevant to the sampling site because it was situated on a 3-story building that is adjacent to streets with a major highway nearby. PCA identified combustion sources as a potential contributor to Hg in Toronto; however, the analysis could not differentiate between vehicular sources or industrial processes. Gasoline and diesel-powered vehicles can be identified based on chemical species/trace element profiles (Landis et al., 2007 and references in Table 2.2), but only criteria air pollutant concentrations were available from the Ontario Ministry of the Environment. The inventory also lacks emissions data on local sources within an urban area that could be impacting the Hg levels at the sampling site. Non-point, urban sources are potentially contributing to the Hg levels at the sampling site because previous studies have reported higher Hg concentrations in urban than rural environments (Rutter et al., 2008). The lack of

atmospheric Hg speciation data (i.e., GEM, PHg<2.5 and RGM concentrations) emitted from the sources also poses a challenge to identify sources of Hg. Hg speciation data from emissions inventory is relevant for source identification because the different physical and chemical properties of Hg species affect their fate and transport. For example, since RGM have a shorter average atmospheric residence time compared to GEM, sources that emit RGM (e.g., coal combustion, Hg cell chlor-alkali plant) would likely affect areas that are close to the source. Landis et al. (2004) found that the percentage of RGM to GEM decreases from 2.1% at a chlor-alkali plant to 1.5% and 1.3% at distances of 350 m and 800 m away, which is evidence of the rapid deposition of RGM and its impacts on local areas.

Without the source emissions data (e.g. criteria air pollutant emissions from the sources) from NPRI, the factors generated by the PMF model would not be able to identify the types of sources contributing to atmospheric Hg levels in Toronto. This is due to the lack of measurements of other chemical/trace element species (e.g., barium, nickel, selenium, vanadium, zinc, etc.), which may be better for characterizing specific types of sources, as illustrated in source apportionment studies of precipitation and particulate matter (Brinkman et al., 2006; Keeler et al., 2006; Lee and Hopke, 2006; Lee et al., 2003). In these studies, mass spectrometry can analyze multiple elements from a single sample, whereas the measurement of different gaseous pollutants requires separate analyzers.

3.4 Contributions to Elevated Hg Events

3.4.1 Analysis of Air Pollutants to Hg Species Ratios

The potential sources contributing to the eight elevated Hg events ([GEM]>20 ng/m^3) in Toronto are likely linked to chemical products, primary metal production, and/or sewage treatment because the average air pollutants to Hg ratios during the elevated Hg events and the entire study period are within the range of ratios for these sources (see Tables 3.2 and 3.4).

Table 3.4: Average NO_2/Hg, $PM_{2.5}$/Hg, and SO_2/Hg (µg of pollutant/ng of Hg) for the annual Hg data set (Dec. 2003 - Nov. 2004) and elevated Hg events ([GEM] > 20 ng/m^3)

	Annual Hg data		**Elevated Hg data**	
	Average	**Standard deviation**	**Average**	**Standard deviation**
NO_2/Hg	11	7.5	6.3	4.5
$PM_{2.5}$/Hg	2.0	3.1	1.4	1.4
SO_2/Hg	1.7	2.8	0.69	0.98
# of measurements	3216		90	

Cement and concrete production and coal combustion likely did not contribute to the measured elevated Hg events. The NO_2/Hg and SO_2/Hg from cement production are on average 43 times and 336 times higher, respectively, than the average ratios from the monitoring site. Similarly, the NO_2/Hg and SO_2/Hg from coal utilities are on average 18 times and 482 times higher, respectively, than the average ratios from the monitoring site. Therefore, it is unlikely for such a large amount of NO_2 and SO_2 deposition to take place in order to reduce the atmospheric ratios from cement production and coal utility sources to those at the monitoring site. These sources potentially contributed to PHg<2.5 levels because of the similar $PM_{2.5}$/Hg. This is further supported by a study that apportioned particulate matter levels in Toronto to a coal-fired power plant in Ontario using the PMF model (Lee et al., 2003).

Atmospheric pollutants ratios have been used in other studies to identify sources contributing to the Hg levels at the sampling site. Similar GEM/CO was reported in Asia and in Oregon, USA confirming that long-range transport of Hg from Asia was responsible for the elevated Hg levels in Oregon (Jaffe et al., 2005); however, the study found major discrepancies between emissions inventory data calculated from emission factors and stack measurements in Asia (Friedli et al., 2004; Jaffe et al., 2005), which can yield different ratios. Emissions inventory data are also reported as an annual average, which might be different from the emissions measured at any point in time (Manolopoulos et al., 2007b). A recent study by Manolopoulos et al. (2007b) found that the NO_2/Hg and SO_2/Hg ratios of the six coal combustion sources located 60 km away were on average two orders of magnitude larger than those at the sampling site, which indicated that those sources were likely not contributing to the measured Hg levels. The reason for this is because it is unlikely that large amounts of deposition would occur between a regional source and the sampling site (Manolopoulos et al., 2007b). Thus, the study attributed the Hg levels at the sampling site to sources located 5 km away, since the ratios were comparable to the sampling site. In the study by Lohman et al. (2006), the SO_2/Hg decreased by 2 from a power plant located ~160 km away to the sampling site near Atlanta, Georgia. In the same study, another power plant located ~30 km away from the sampling site had a SO_2/Hg 1.1 to 1.6 times higher than that of the sampling site, which illustrates that SO_2 losses are generally minor.

3.4.2 Back Trajectory Modeling

To investigate whether the meteorological conditions during the elevated Hg events favored the transport of Hg from the regional sources to the sampling site in Toronto, 48-hour back trajectories corresponding to the period of the elevated Hg episodes were generated using

the HYSPLIT (HYbrid Single-Particle Lagrangian Integrated Trajectory) model (Drexler and Rolph, 2003; Rolph, 2003). There were a total of eight elevated Hg events, defined as a time period where GEM concentrations were above 20 ng/m^3, throughout the entire monitoring campaign. The elevated GEM events lasted from a few hours to 1-2 days.

The back trajectories at starting heights of 15, 50 and 500 m for each elevated Hg event are shown in Figures 3.2 to 3.7. The 48-hour back trajectories during the Jan 23rd event (Figure 3.2) illustrates that the trajectories passed through Thunder Bay, where a fossil fuel power generation facility is located. Figure 3.3(a) shows that the trajectory paths for the three starting heights are different for the Feb 28th event and did not appear to pass through any regional point sources. The May 25th event shown in Figure 3.3(b) shows that the lower starting height trajectories (15 m and 50 m) passed through point sources located in Toronto (Sewage treatment), Pickering (Sewage treatment), Whitby (Metal production), Nanticoke (Power generation), Haldimand County (Metal production) and Woodstock (Cement and concrete). Back trajectories generated for June 8th (Figure 3.4), June 28th (Figure 3.5) and July 19th (Figure 3.6) events appeared to pass through many point sources in southern Ontario, including a power generation facility, cement and concrete manufacturing, sewage treatment, and metal production. The June 8th trajectories extend to the state of Ohio and Indiana in the US, which contains industrial areas and populated urban centers. Back trajectories generated for the Detroit sampling site also found that the site was influenced by regional sources in Ohio and Indiana as well (Lynam and Keeler, 2005). Back trajectories during the elevated Hg event on Sept. 7th (Figure 3.7(a)) did not appear to originate from sources in Ontario. The back trajectories on Oct. 20th (Figure 3.7(b)) passed through two sewage treatment facilities in Toronto and Pickering and a primary metals facility.

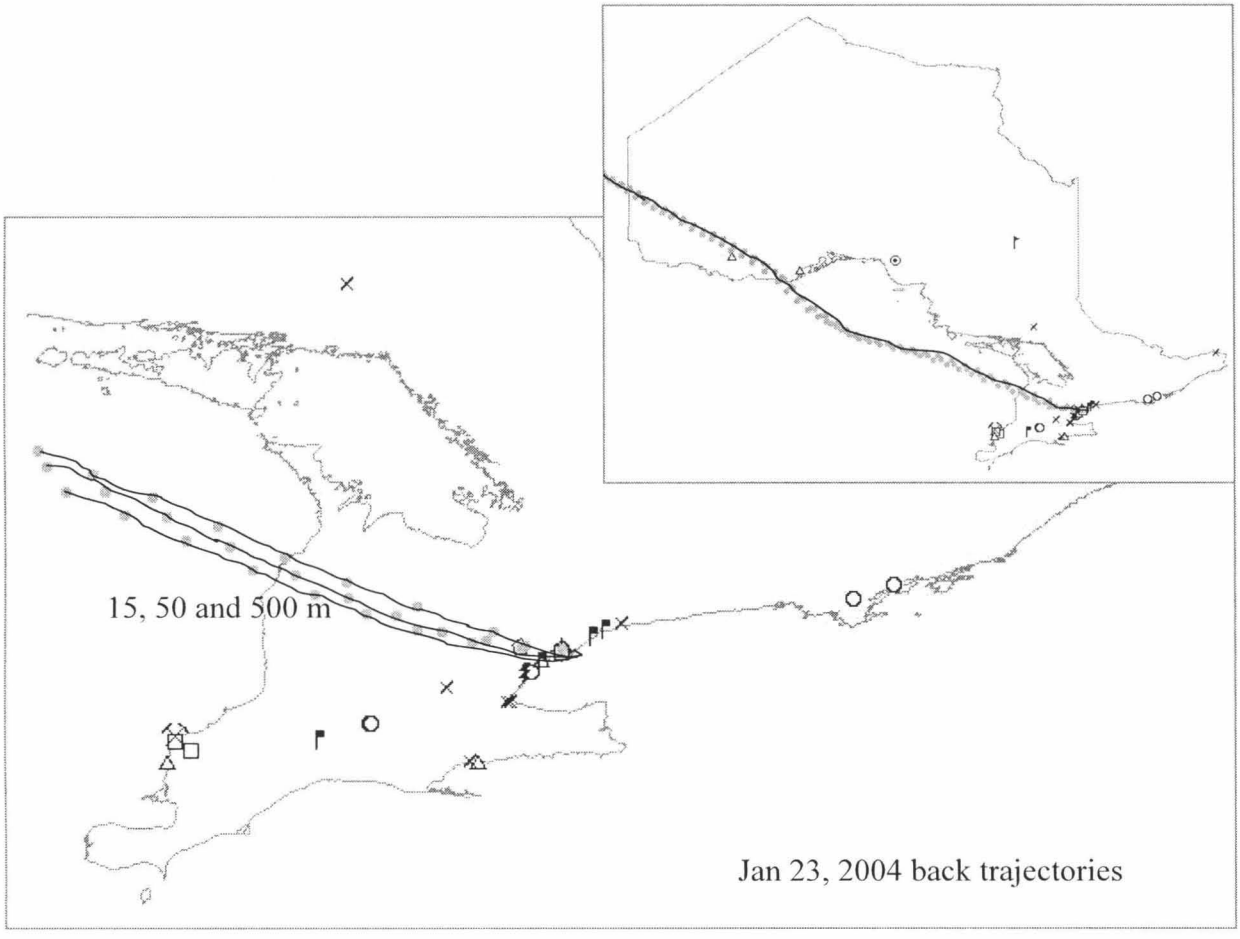

- Weather station
- Air pollutant sampling site
- Hg sampling site
- Sewage waste treatment
- Pulp and paper
- Metals
- Coal utility
- Other power generation
- Non-Fe metal
- Electrical products
- Chemical products
- Cement and concrete

Figure 3.2: Back trajectories at starting heights of 15, 50 and 500 m for Jan 23, 2004 elevated Hg event

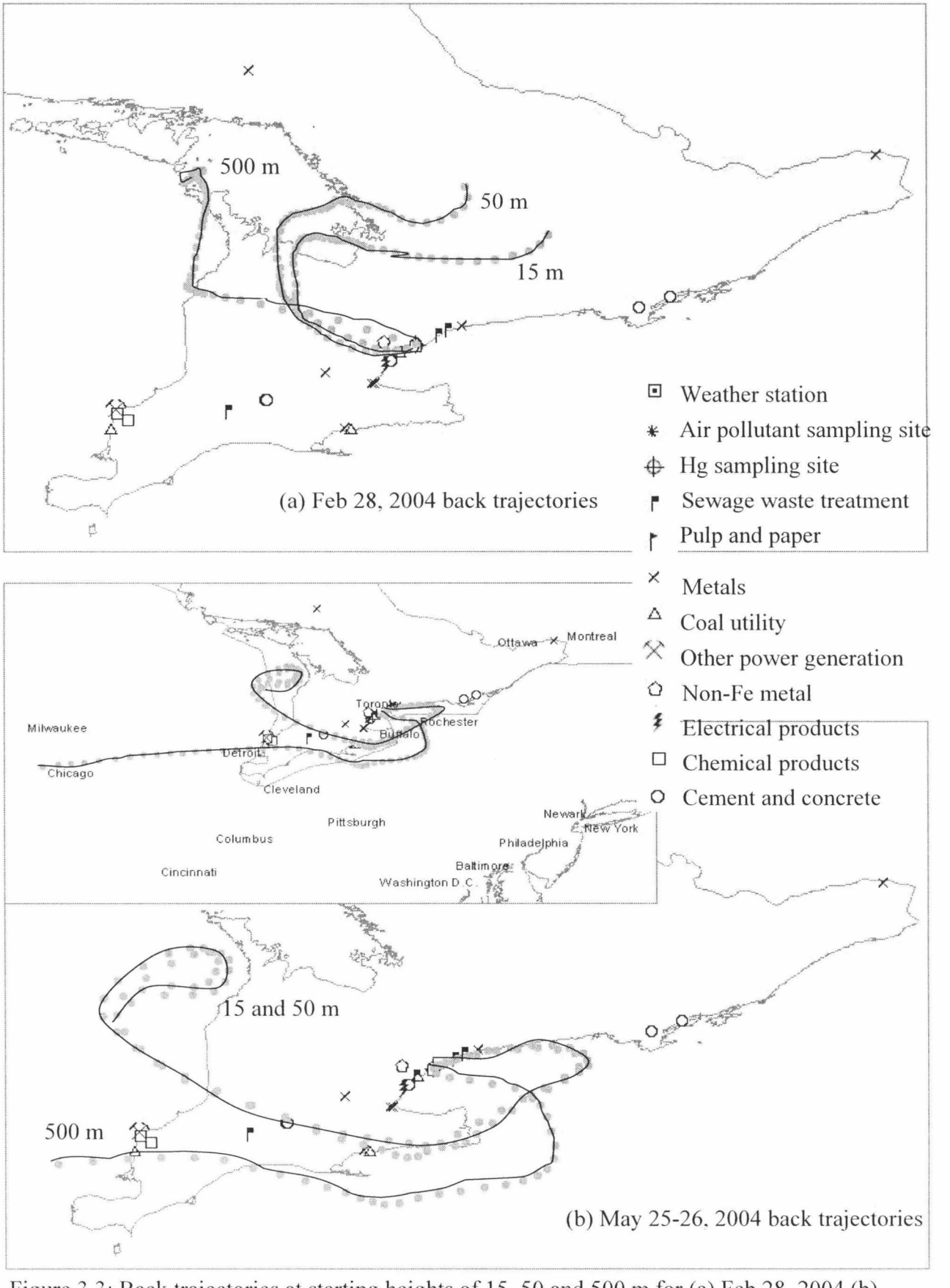

Figure 3.3: Back trajectories at starting heights of 15, 50 and 500 m for (a) Feb 28, 2004 (b) May 25-26, 2004 elevated Hg event

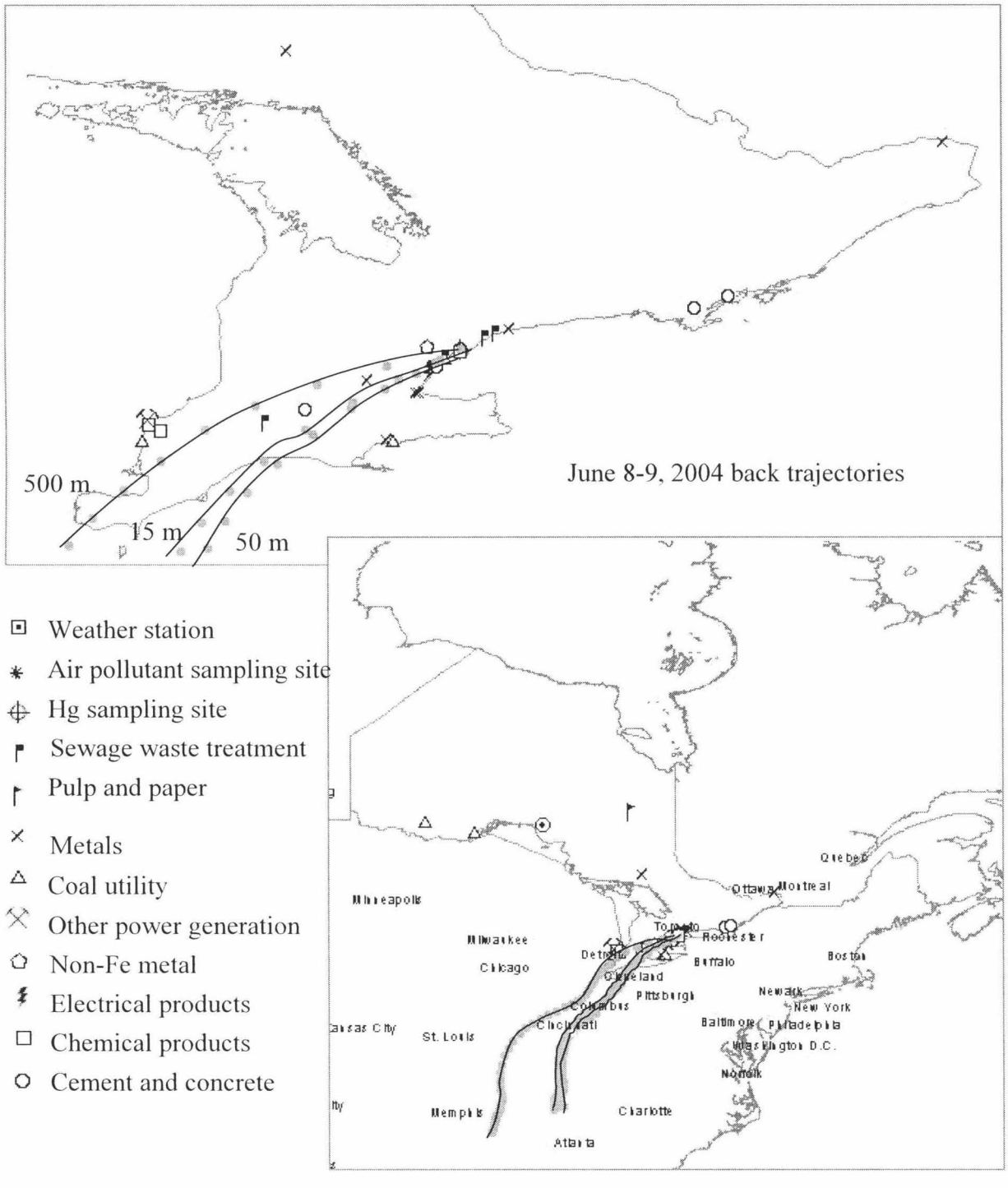

Figure 3.4: Back trajectories at starting heights of 15, 50 and 500 m for June 8-9, 2004 elevated Hg event

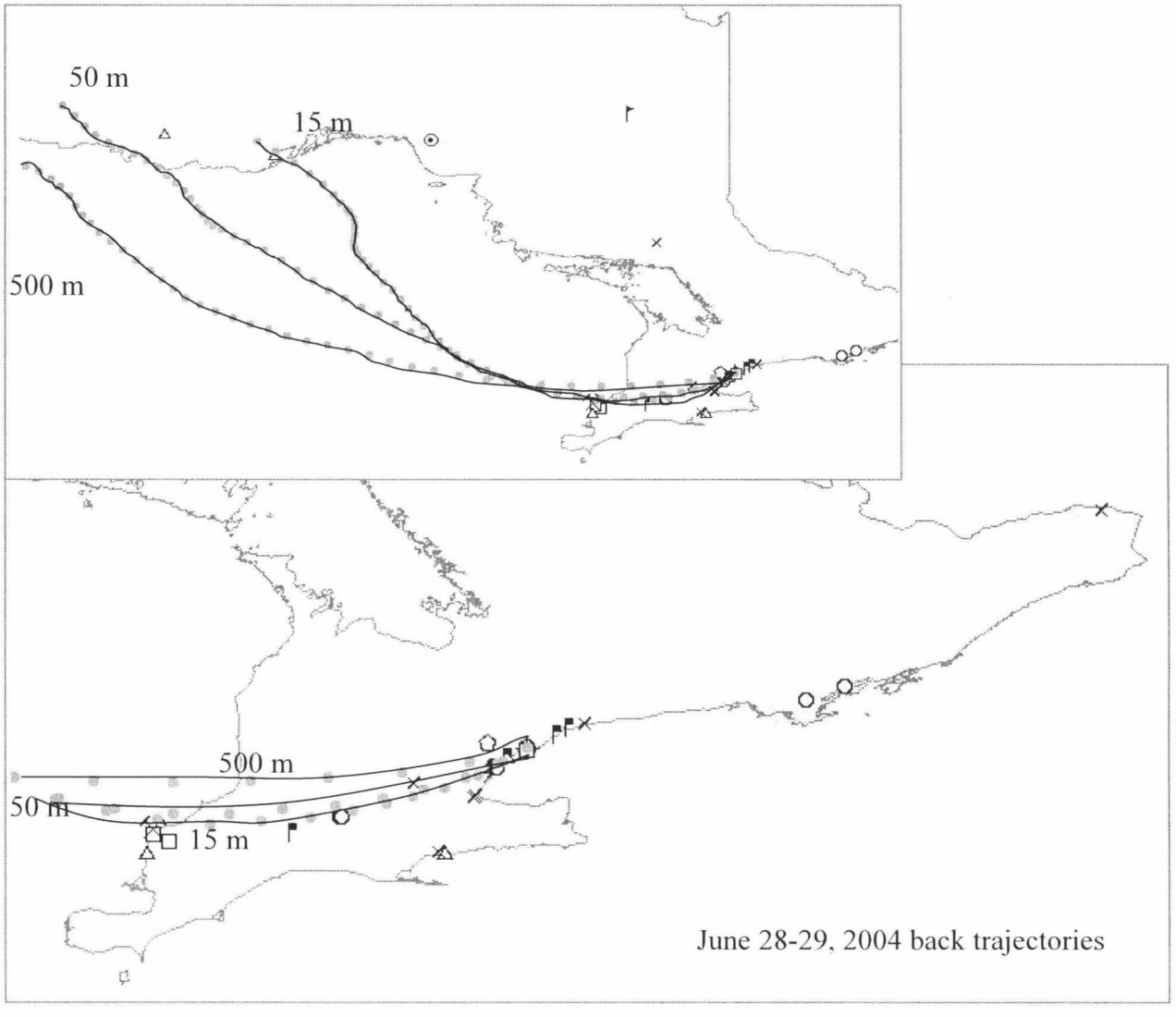

- Weather station
- Air pollutant sampling site
- Hg sampling site
- Sewage waste treatment
- Pulp and paper
- Metals
- Coal utility
- Other power generation
- Non-Fe metal
- Electrical products
- Chemical products
- Cement and concrete

Figure 3.5: Back trajectories at starting heights of 15, 50 and 500 m for June 28-29, 2004 elevated Hg event

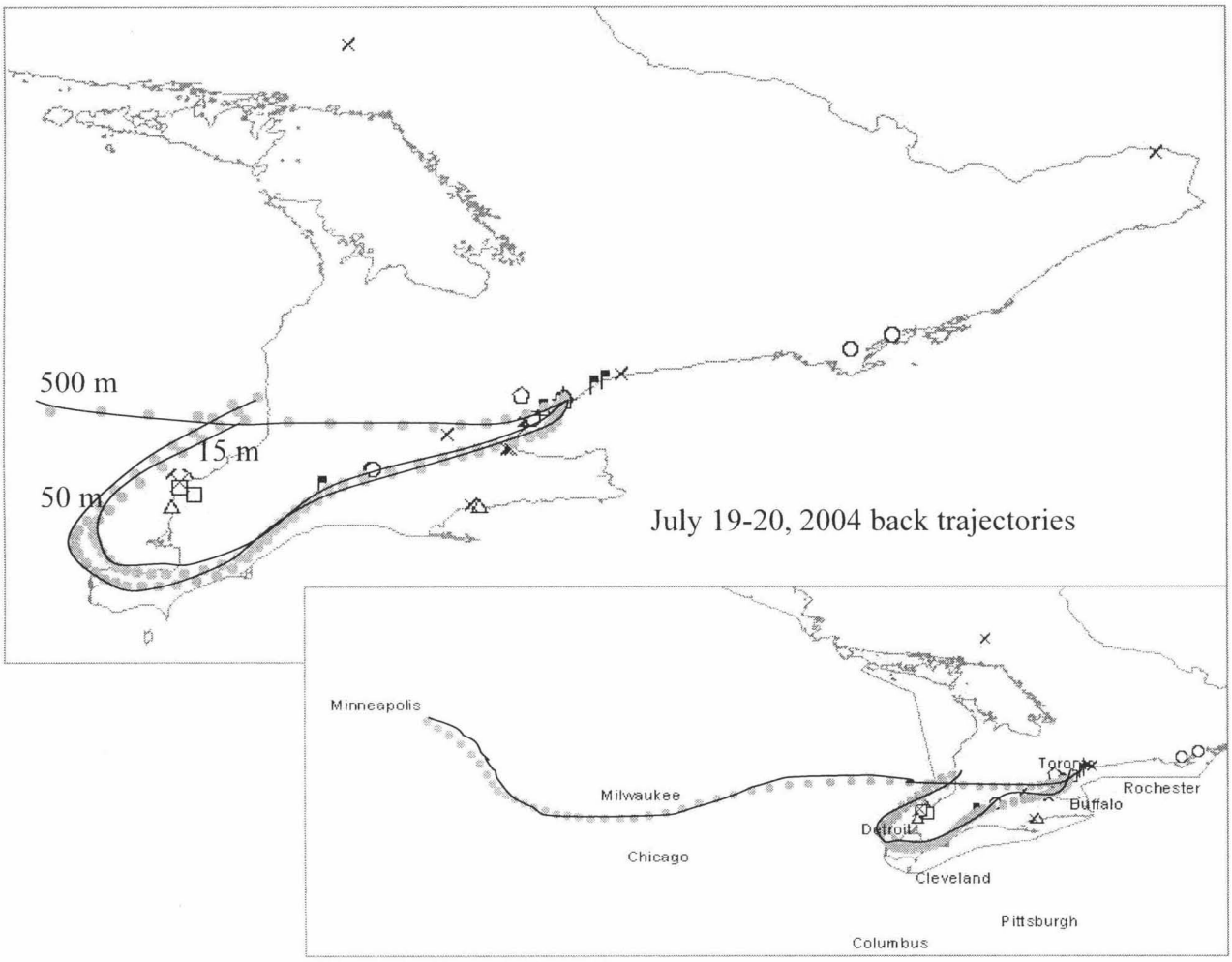

- Weather station
- Air pollutant sampling site
- Hg sampling site
- Sewage waste treatment
- Pulp and paper
- Metals
- Coal utility
- Other power generation
- Non-Fe metal
- Electrical products
- Chemical products
- Cement and concrete

Figure 3.6: Back trajectories at starting heights of 15, 50 and 500 m for July 19-20, 2004 elevated Hg event

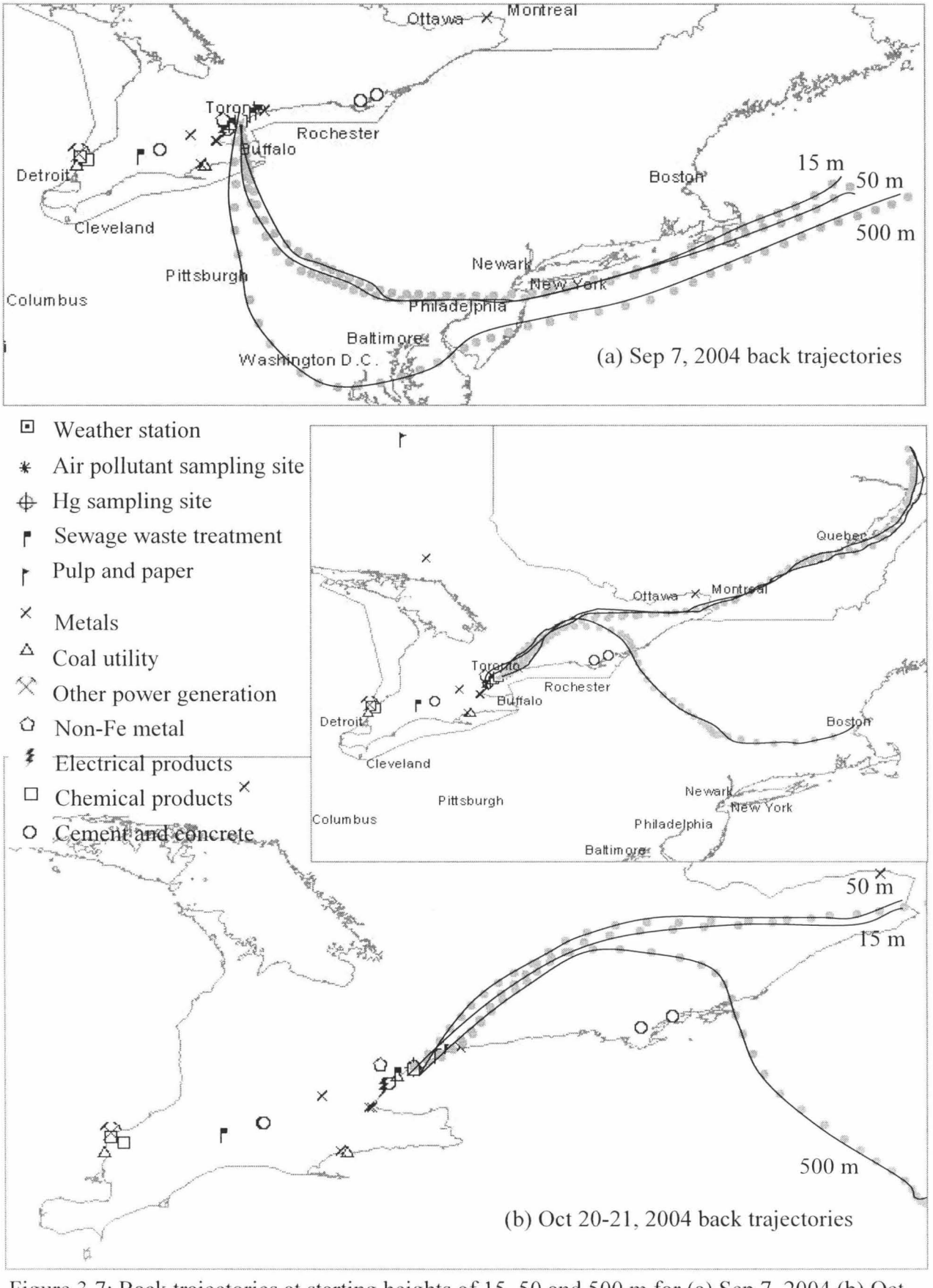

Figure 3.7: Back trajectories at starting heights of 15, 50 and 500 m for (a) Sep 7, 2004 (b) Oct 20-21, 2004 elevated Hg event

3.4.2.1 Back Trajectory Modeling Uncertainties

Back trajectory modeling has been widely used to locate sources of pollutants (Lee et al., 2003; Liu et al., 2007; Lynam and Keeler, 2005). However, recent literature on air pollution modeling (Arain et al., 2007; Ryaboshapko et al., 2007) and our analysis have found that trajectory modeling using a coarse meteorological data resolution is not suitable for simulating pollutant transport through an urban atmosphere, such as in downtown Toronto. The airflow at lower elevations, such as the 15 m and 50 m starting trajectory heights, are influenced by buildings that are southwest of the Hg sample inlet as shown in Figure 3.8. Unless the meteorological data input to the trajectory model fully accounts for the effects of urban structure on wind fields, there would be uncertainties as to whether the pollutants were transported to the sampling site via the trajectory pathway. The EDAS 40 km meteorological data used in the HYSPLIT model is sufficient to resolve regional point sources, as this was used in Lynam and Keeler's study (2005) to identify sources within 30-40 km of the Detroit sampling site. However, this study requires finer meteorological data resolution to resolve potential urban sources near downtown Toronto.

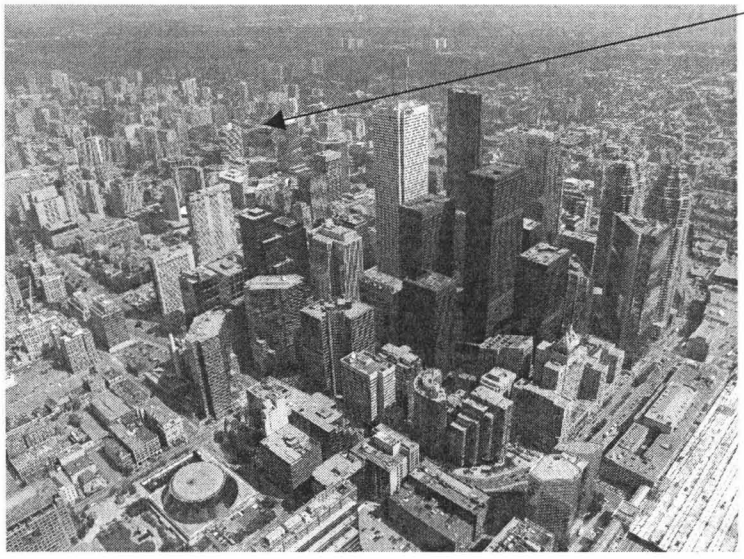

Figure 3.8: Aerial photo of downtown Toronto in 2004 (northeast view) to illustrate the potential impacts buildings have on the airflow through downtown Toronto.

3.4.3 Analysis of Atmospheric Hg Species Ratios

RGM/PHg<2.5 and wind directions during the elevated GEM events observed in Toronto were analyzed to determine the regional sources impacting the site and confirm back trajectory modeling results. Figure 3.10 illustrates plots of RGM/PHg<2.5 ratios and wind directions during six of the elevated Hg events, in which meteorological data was available at the sampling site (i.e., beginning of May 2004). The wind directions shown in Figure 3.10 were measured at two weather stations. WD1 refers to the wind directions measured at the sampling site at a height of 14 m, whereas WD2 refers to the wind directions measured at the Toronto Island Airport at a height of 76.5 m. Toronto Island Airport is located in Lake Ontario, south/southwest of the sampling site. The wind directions measured at Toronto Island Airport are relevant to the analysis because it can be used to verify the trajectory paths generated from the HYSPLIT model, since the previous aerial photo suggests that the buildings were affecting the airflow from the southwest direction to the Hg sample inlet. During May to December 2004, most of the winds originated from the east and southwest directions at the Toronto Island Airport station and from the northeast and southwest directions at Ryerson University as shown in the wind direction frequency distributions in Figure 3.9.

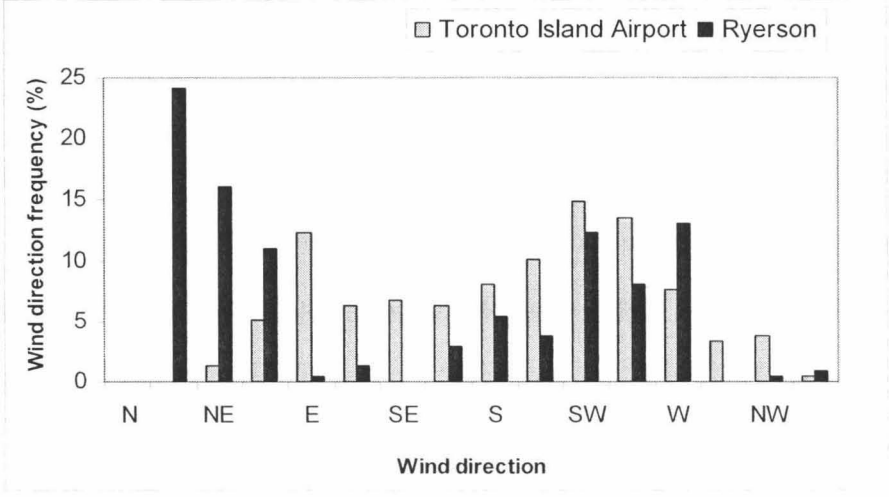

Figure 3.9: Wind direction frequency distribution based on daily averaged wind directions measured at Ryerson University and Toronto Island Airport between May and December 2004.

Figure 3.10 illustrates that only the elevated Hg events on June 8th, July 19th and Oct 20th were likely affected by Hg emissions from local/regional sources in Ontario. On the June 8th episode (Figure 3.10(b)), the wind directions at the sampling site and Toronto Island Airport remained constant from the southwest direction as the RGM/PHg<2.5 decreases. As a result, it is probable that the elevated GEM concentrations on June 8th are due to sources located southwest of the sampling site. The average wind speed measured at Ryerson University during the June 8th episode was 1.3 ± 0.8 m/s, which suggests that the Hg plume could be transported by wind to the sampling site. Back trajectory results also confirm that the airflow passed through several sources southwest of the sampling site.

Similar results were also observed for the elevated GEM concentrations on July 19th (Figure 3.10(d)). The wind directions measured at both stations on the July 19th were consistent with each other; both graphs illustrate the wind direction was constantly from the southwest as the RGM/PHg<2.5 decreases. Furthermore, back trajectory modeling confirmed that the airflow passed through several sources located in southwestern Ontario. However, the average wind speed during the July 19th episode was only 0.54 ± 0.54 m/s, which suggests that the Hg plume might not have been transported by wind from another location. It is possible that daytime Hg emissions near the sampling site were trapped in a stable atmosphere during nighttime radiative inversion, which allowed for the gas partitioning process that converts RGM to PHg<2.5 to occur. Radiative inversion might lead to elevated pollutant levels in the troposphere because the radiation of heat from the ground surface at night produces a colder layer of air near the ground than the air at higher elevations, which prevents the vertical transport and dispersion of pollutants (Zoras, 2006). Atmospheric stability has been estimated based on measurements of

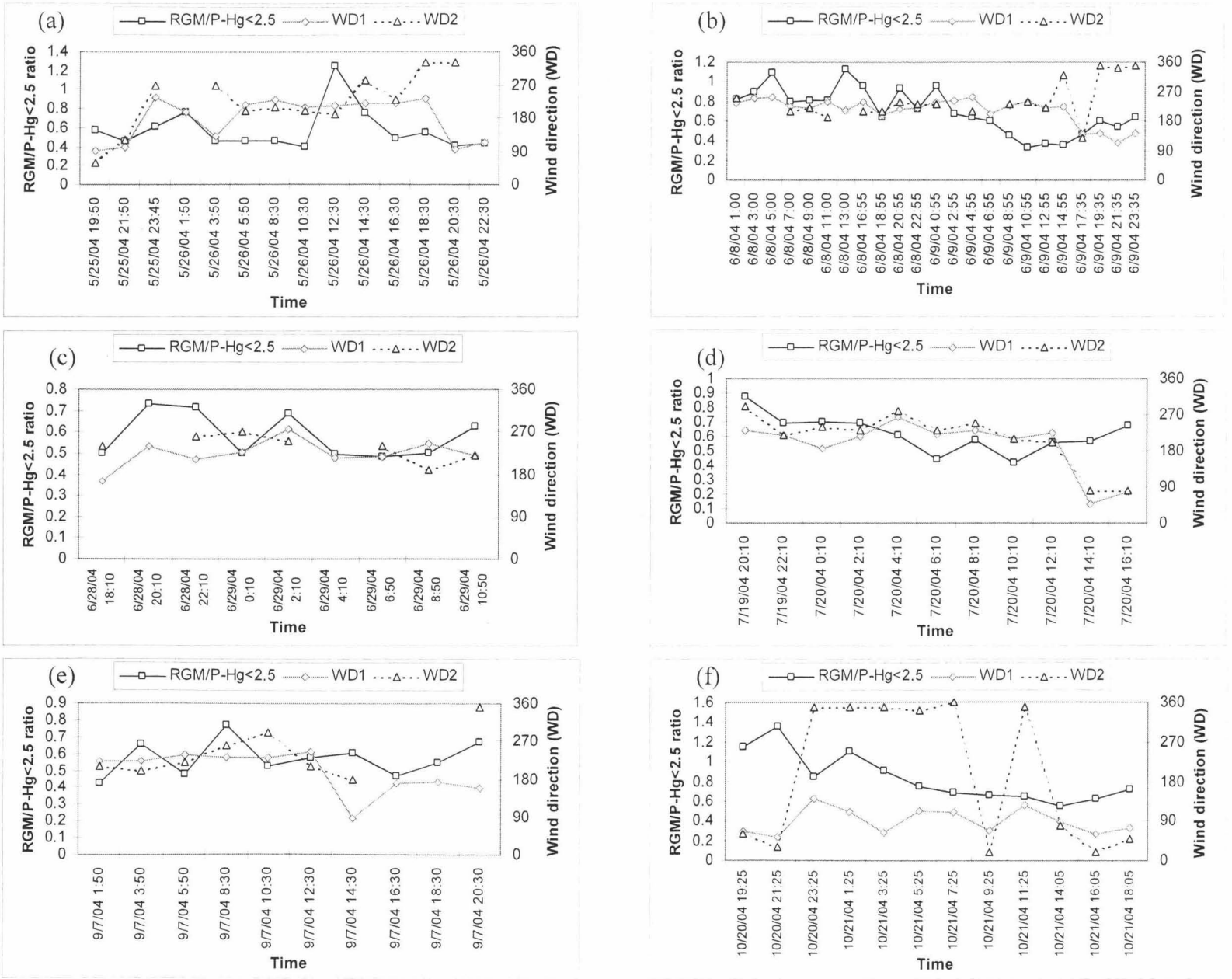

Figure 3.10: RGM/PHg<2.5 and wind directions measured at two weather stations in downtown Toronto during elevated GEM events. (a) May 25-26, (b) June 8-9, (c) June 28-29, (d) July 19-20, (e) Sep 7, (f) Oct 20-21; WD1 = wind direction at sampling site; WD2 = wind direction at Toronto Island Airport.

incoming solar radiation, cloud cover and wind speeds (Pasquill, 1961; Turner, 1964; Zoras et al., 2006). The Hg and NO_x concentration peaks, calm winds (e.g., 0-0.5 m/s), and clear skies (e.g. average cloud cover in July was ~15%, NASA, 2008) observed during the overnight hours suggest that radiative inversion might have occurred. However, radiative inversions are more common in the winter due to the potential for snow cover on the ground, which cools the layer of air adjacent to the ground surface (Elminir, 2007; Zoras, 2006).

The elevated GEM levels during Oct 20th (Figure 3.10(f)) were potentially impacted by primary metals facilities and sewage treatment plants, which were identified from the analysis of atmospheric pollutants ratios. The decreasing RGM/PHg<2.5 coincided with the easterly winds measured at Ryerson University, which is consistent with the back trajectories that passed through a primary metals facility and two sewage treatment plants located east of the sampling site. The average wind speed was 3.3 ± 1.3 m/s, which illustrates that wind was potentially transporting Hg plumes emitted from these sources to the sampling site.

Figure 3.10(a), (c) and (e) illustrates that decreasing RGM/PHg<2.5 were not observed on the May 25th, June 28th and Sep. 7th elevated GEM events. Therefore, it is uncertain whether the Hg plume from the sources identified by back trajectories was transported by wind to the sampling site during those three events. The back trajectories only track the path of air, which is not necessarily the same path as an Hg plume. The wind direction corresponding to the maximum Hg level during the three elevated Hg events was southwest, which suggests that there could be urban sources of Hg near the sampling site located in the southwest direction.

The Hg speciation study conducted by Lynam and Keeler (2005) used RGM to PHg<2.5 ratios and wind direction data to determine whether regional sources were affecting the Hg levels measured in Detroit. In that study, a significantly lower RGM/PHg<2.5 was observed in the

south to southwest direction, where there were industrial areas and populated urban centers located in Ohio and Indiana, than in the east direction (Lynam and Keeler, 2005). These sources were also confirmed by back trajectory modeling using HYSPLIT in their study.

3.5 Correlation Analysis Results

Correlation analysis was performed on the entire data set obtained from the Toronto site for each season and the results are listed in Table 3.5. The data set was separated into different seasons because ozone is affected by meteorological variables, such as solar radiation and temperature (Kim and Kim, 2001). Table 3.5 illustrates that correlations between Hg species and ozone are either weak or not significant in the winter. There is also a weak relationship between GEM and RGM, as well as RGM and nitrogen oxides and SO_2. In the spring, there is a moderate relationship between GEM and RGM (see Table 3.5). GEM and O_3 were found to be weakly anti-correlated, and RGM and O_3 were weakly correlated, which indicates the depletion of GEM by O_3, converting GEM to RGM. The weak Hg-O_3 correlations do not necessarily indicate that photochemical reactions did not occur because the oxidation of GEM to RGM is a slow process (Han et al., 2004; Manolopoulos et al., 2007a; Sillman et al., 2007). Only weak correlations between RGM, nitrogen oxides and SO_2 were observed. These results suggest that springtime RGM concentrations at the sampling site can be produced from both direct emission or indirectly from photochemical processes. The correlation results for the summer demonstrated that photochemical reactions with ozone played a bigger role in the production of RGM compared to other seasons. This is due to the significant negative correlation between GEM and O_3 and strong positive correlation between RGM and O_3. The correlations between GEM and RGM as well as RGM and SO_2 indicate direct emission of RGM is still a potential source.

Table 3.5: Correlation coefficients (Pearson r) between Hg species and criteria air pollutants concentrations for each season between December 2003 and November 2004

Winter									
	PHg<2.5	*RGM*	*CO*	*NO*	*NO_2*	*NOx*	*O_3*	*$PM_{2.5}$*	*SO_2*
GEM	0.043	0.145**	(0.094)*	0.029	0.075*	0.057	(0.0127)**	0.069	0.014
PHg<2.5		0.416**		0.067	0.196**	0.145**	0.100**	0.023	0.012
RGM				(0.01)	0.068	0.031	0.066	0.014	0.088*
Spring									
	PHg<2.5	*RGM*	*CO*	*NO*	*NO_2*	*NOx*	*O_3*	*$PM_{2.5}$*	*SO_2*
GEM	0.446*	0.269**	0.108**	0.056	0.152**	0.112*	(0.141)**	0.132**	0.092**
PHg<2.5		0.343**	(0.001)	0.007	0.053	0.03	0.116**	0.088**	0.088**
RGM			(0.04)	(0.056)	0.001	(0.034)	0.109**	(0.27)	0.093**
Summer									
	PHg<2.5	*RGM*	*CO*	*NO*	*NO_2*	*NOx*	*O_3*	*$PM_{2.5}$*	*SO_2*
GEM	0.560**	0.410**	0.364**	0.204**	0.342**	0.300**	(0.198)**	0.232**	0.033
PHg<2.5		0.714**	0.076	(0.01)	0.087**	0.039	0.328**	0.278**	0.179**
RGM			0.098	(0.073)*	0.069*	(0.006)	0.416**	0.358**	0.380**
Fall									
	PHg<2.5	*RGM*	*CO*	*NO*	*NO_2*	*NOx*	*O_3*	*$PM_{2.5}$*	*SO_2*
GEM	0.653**	0.484**	0.259**	0.213**	0.226**	0.241**	(0.333)**	0.053	0.081**
PHg<2.5		0.645**	0.175**	0.194**	0.171**	0.205**	(0.141)**	0.052	0.163**
RGM			0.152**	0.087**	0.204**	0.138**	0.085**	0.293**	0.290**

Parentheses indicate negative correlations
* indicate significant correlations ($p<0.05$)
** indicate significant correlations ($p<0.01$)

The ozone concentrations in the spring and summer are statistically higher than winter and fall ($p<0.0005$, Wilcoxon Rank Test), which led to stronger correlations between RGM and O_3 in the spring and summer. The strong GEM-RGM correlations along with the significant correlations between RGM, nitrogen oxides and SO_2 in the fall illustrate that RGM production is mainly driven by direct source emission of RGM. Although the oxidation of GEM by ozone does occur as evident by the negative GEM-O_3 correlation, the strong RGM-O_3 correlation in the summer was not observed in the fall.

Correlation analysis was also conducted on the Hg species and criteria air pollutant concentrations corresponding to the elevated GEM events (GEM concentration > 20 ng/m^3). The model predicted correlations of the air pollutants from Sillman et al.'s study (2007) were used to investigate whether direct emissions or photochemical processes dominate the production of RGM. Almost all the elevated Hg events exhibited strong correlations between GEM and RGM, except for the Feb 28th and Sep 7th events, in which the correlations were not significant.

Among the correlated GEM-RGM events, only two events on May 25th and June 8th showed strong correlations between RGM and O_3 ($r = 0.54$ to 0.65, $p<0.05$) and anti-correlations between RGM and nitrogen oxides ($r = -0.11$ to -0.26). On the May 25th event, RGM and ozone concentrations peaked during the noon hour, which indicated the occurrence of photochemical reactions involving ozone and GEM. On the June 8th event, the Ontario Ministry of the Environment (2008) issued smog advisories for the City of Toronto, which indicated increase levels of smog precursors, such as ozone and fine particulate matter. The levels of RGM and ozone peaked during noon and overnight hours (i.e., bimodal trend) on the June 8th event, which suggests the role of ozone on the oxidation of GEM in the afternoon and the potential transport of oxidizing air masses from distant sources at night. The latter point is supported by back trajectory modeling, RGM/PHg<2.5 and wind analysis results, which traced the airflow to industrial and urban areas located in Ohio. The study by Lynam and Keeler (2005) also found that the industrial and urban sources in Ohio were impacting the Detroit site. It is possible that distant sources emit Hg and nitrogen oxide during daytime, which then formed ozone in the presence of sunlight, and thus produced an oxidizing air mass that converts emissions of GEM to RGM.

The June 28th and July 19th events showed strong anti-correlations between RGM and O_3 ($r = -0.53$ to -0.61, $p<0.07$) and moderate correlations between RGM and nitrogen oxides ($r = 0.37$ to 0.51). However, the diurnal nitrogen oxides trends do not suggest vehicle emission sources because nitrogen oxides concentrations peaked during the overnight and early morning hours, but the emissions might be related to other combustion processes, such as industrial processes (Liu et al., 2007). Analysis of air pollutants to Hg ratios and back trajectories indicate that sewage treatment and metal production are potential sources for both events. But a decreasing RGM/PHg<2.5 was not observed on the June 28th event to suggest that Hg plumes from the sources were transported to the sampling site. The July 19th event could either be affected by regional sources due to the declining RGM/PHg<2.5, or the build up of pollutants emitted from nearby sources during nighttime radiative inversion. The Hg and NO_x concentration peaks and the low wind speeds observed during the overnight hours might be related to radiative inversion, which produces a stable atmosphere that prevents the dispersion of pollutants.

Weak RGM-SO_2 correlations were observed for all the elevated Hg events. This supports the previous model/data analysis results, i.e., coal combustion sources were not the major contributor to the Hg levels at the Toronto site. However, coal combustion emits nitrogen oxides and volatile organic compounds that can lead to the formation of ozone, which might explain the elevated O_3 levels on the June 8th event. A summary of the modeling/data analysis results and interpretation for all the elevated Hg events are shown in Table 3.6.

Several other studies have examined the relationship of Hg species and ozone to determine whether photochemistry has an effect on Hg species levels and distributions. The method of analysis that is often used is correlation analysis between Hg species and ozone (Han

et al., 2004; Kim and Kim, 2001; Lindberg and Stratton, 1998; Lynam and Keeler, 2005; Sillman et al., 2007). Correlation between RGM and ozone levels was observed in the studies conducted by Lindberg and Stratton (1998) and Lynam and Keeler (2005), and a weak anti-correlation between GEM and ozone was also reported in Lynam and Keeler's study (2005). The studies by Han et al. (2004) in New York and Kim and Kim (2001) in Seoul did not find significant positive correlations between measured RGM and O_3 concentrations. Correlation analysis of model-predicted GEM and RGM concentrations were also used to identify direct emission sources or photochemical production of RGM (Sillman et al., 2007). In the study by Sillman et al. (2007), the CMAQ (Community Multi-scale Air Quality) model, which is generally used to study the transport and transformation of pollutants by chemical reactions, was modified to model gas-phase species and photochemical processes involving ozone, nitrogen oxides, organics, sulfur and mercury on a regional scale. The model results predicted an anti-correlation between GEM and RGM when RGM is formed from photochemical reactions, and a positive correlation between GEM and RGM when direct sources are emitting RGM. It also predicted that a strong correlation between RGM and ozone is likely when concentrations of ozone and its precursors (NO_x, VOC) are elevated (which was observed in this study), and correlations between RGM and SO_2 or reactive nitrogen are indicators of direct emissions of RGM.

Although these results provide some insight about sources of RGM, there are significant uncertainties with using models to predict RGM concentrations that have been discussed in literature. A comparison study (Ryaboshapko et al., 2007) of various atmospheric Hg models found that predicted and measured concentrations differed by a factor of 1.35-1.5 for GEM and a factor of 10 for RGM and suggested that the large RGM discrepancies were mainly due to an incomplete understanding of the various chemical processes of RGM in the atmosphere (e.g.,

oxidation from GEM by various oxidants, RGM adsorption onto particulates, and wet deposition (Lindberg and Stratton, 1998), reduction of RGM to GEM in a mercury plume (Edgerton et al., 2006; Lohman et al., 2006)). Although chemical models are effective at estimating hydroxyl and ozone concentrations, which are involved in GEM oxidation, the oxidation of GEM by reactive halogens has not been modeled extensively (Lin et al., 2006). Thus, the use of the modeling results by Sillman et al. (2007) that attempted to differentiate between primary and secondary production of RGM could be very inaccurate if these RGM processes were not included in the model. The modeling study also attributed the uncertainties to the use of coarse resolution data in the models, which was a major issue raised from the back trajectory modeling results of the downtown Toronto area and a NO_2 pollution study in the Toronto-Hamilton area (Arain et al., 2007). Furthermore, measurements of Hg in urban areas are prone to large spatial variability as evident by GEM concentrations measured at two different heights at the same urban location (St. Denis et al., 2006) and Hg emissions from urban surfaces (Eckley and Branfireun, 2008).

Table 3.6: Summary of the elevated GEM events analyses and interpretation of results

	Atmospheric pollutant ratios			Interpretation of air pollutant ratios	Back trajectory modeling			Decreasing RGM/PHg<2.5?		Measured wind direction during max. Hg levels	Interpretation of back trajectory, RGM/PHg<2.5 and wind analysis	Strong positive correlations?				Interpretation of correlations
Elevated GEM events	NO_2/Hg	$PM_{2.5}$/Hg	SO_2/Hg		Sources that trajectories passed through	Local (<50 km) or Regional	Direction of source relative to sampling site	From SW direction	From E direction			RGM-O_3	RGM-NOx	RGM-SO_2	GEM-RGM	
23-Jan-04	0.9-20	0.04-1.1	0-0.5	chemical production, metals processing, sewage treatment are potential sources	Non-Fe metal Coal utility	Local Regional	NW NW			N/A	Uncertain whether Hg plume was transported by wind from the sources to sampling site and location of urban sources				Yes	Direct emissions of RGM; coal combustion unlikely
28-Feb-04	3.6-9.8	0.16-0.37	0.11-0.74	chemical production, metals processing, sewage treatment are potential sources	Coal utility Sewage treatment Non-Fe metal	Local Local Local	SW SW NW			N/A	Uncertain whether Hg plume was transported by wind from the sources to sampling site and location of urban sources					Inconclusive about sources of RGM; coal combustion unlikely
25-May-04	0.9-13.9	0.02-4.9	0-4.1	chemical production, metals processing, sewage treatment are potential sources	Sewage treatment (2) Metals Coal utility Metals Cement & concrete	Local Local Regional Regional Regional	E E SW SW SW			SW	Uncertain whether Hg plume was transported by wind from the sources to sampling site; unidentified urban sources from SW is possible	Yes RGM peaked during noon and overnight hours; O_3 peaked at noon			Yes	Direct emissions of RGM and presence of oxidizing atmosphere at noon hour; coal combustion unlikely, but could emit precursors of O_3
8-Jun-04	0.68-10.8	0.41-7.6	0-4.1	chemical production, metals processing, sewage treatment are potential sources	Coal utility Sewage treatment Cement & concrete Electrical products Cleveland, Columbus, Cincinnati, US	Local Local Local Local Regional	SW SW SW SW SW	Yes		SW	Local/regional sources identified by back trajectory are potential sources contributing to the sampling site	Yes RGM and O3 peaked at noon and overnight hours; reported smog day by Ontario MOE			Yes	Direct emissions of RGM and transport of oxidizing air mass at night; coal combustion unlikely, but could emit precursors of O3

Table 3.6 *continued*: Summary of the elevated GEM events analyses and interpretation of results

	Atmospheric pollutant ratios			Interpretation of air pollutant ratios	Back trajectory modeling			Decreasing RGM/PHg<2.5?		Measured wind direction during max. Hg levels	Interpretation of back trajectory, RGM/PHg<2.5 and wind analysis	Strong positive correlations?				Interpretation of correlations
Elevated GEM events	NO_2/Hg	$PM_{2.5}$/Hg	SO_2/Hg		Sources that trajectories passed through	Local (<50 km) or Regional	Direction of source relative to sampling site	From SW direction	From E direction			RGM-O_3	RGM-NOx	RGM-SO_2	GEM-RGM	
28-Jun-04	2.3-14.6	0-1.9	0.11-2.1	chemical production, metals processing, sewage treatment are potential sources	Coal utility Sewage treatment Cement & concrete Electrical products Metals Cement & concrete Sewage treatment Other electric power Coal utility	Local Local Local Local Regional Regional Regional Regional Regional	SW SW SW SW SW SW SW SW NW			WSW	Uncertain whether Hg plume was transported from the sources to sampling site; unidentified urban sources from WSW is possible	Yes			Yes RGM, PHg<2.5, and NOx peaked in the overnight hours; thus local vehicular emissions is an unlikely source	Combustion sources, but likely not related to vehicle emissions and coal combustion
19-Jul-04	2.6-11.8	0.65-3.2	0-4.4	chemical production, metals processing, sewage treatment are potential sources	Metals Cement & concrete Sewage treatment Detroit, US	Regional Regional Regional Regional	SW SW SW SW	Yes Little to no wind was observed		WSW	Analysis suggests regional sources are contributing to the sampling site, but the lack of wind could suggest that Hg emissions came from urban sources in WSW	Yes			Yes RGM, PHg<2.5 and NOx peaked in the early morning hours; thus local vehicular emissions is an unlikely source	Combustion sources, but likely not related to vehicle emissions and coal combustion
7-Sep-04	1.9-23.6	0-3.7	0.21-2.93	chemical production, metals processing, sewage treatment are potential sources	Philadelphia, New York, US	Regional	S and SE			SW	Uncertain whether Hg plume was transported from the sources to sampling site; unidentified urban sources from SW is possible					Inconclusive about sources of RGM; coal combustion unlikely
20-Oct-04	0.6-12.7	0.11-1.92	0	chemical production, metals processing, sewage treatment are potential sources	Sewage treatment (2) Metals	Local Local	E E		Yes	E	Local sources identified by back trajectory are potential sources contributing to the sampling site				Yes	Direct emissions of RGM; coal combustion unlikely

4. Conclusions and Significance of Findings

4.1 Conclusions

- ***PMF and PCA results***: Model results of the annual (December 2003 to November 2004) data and National Pollutant Release Inventory (NPRI) emissions data suggest industrial processes (chemical production, metal production, sewage treatment), rather than coal combustion and cement and concrete production, were the major contributors to measured Hg levels in downtown Toronto. Both models also identified factors that cannot be characterized using NPRI emissions data.

- ***Atmospheric Pollutants Ratio Analysis (NO_2/Hg, $PM_{2.5}$/Hg, SO_2/Hg)***: Ratios of air pollutants to Hg at the sampling site during the elevated GEM events (i.e., GEM concentrations > 20 ng/m^3) are similar to those from chemical manufacturing, metal production, and sewage treatment facilities, and not coal combustion or cement and concrete production. The large NO_x/Hg and SO_2/Hg from coal combustion and cement production relative to those of the sampling site indicate that these sources are likely not contributing to Hg levels in Toronto because of the large NO_x and SO_2 deposition required to reduce the NO_x/Hg and SO_2/Hg. Since chemical manufacturing plants are located more than 300 km away from the Hg sampling site, the use of mercury-containing products in an urban city is potentially a source of Hg.

- ***Ratio Analysis (RGM/PHg<2.5) and Back Trajectory results:*** Decreasing RGM/PHg<2.5 during 2 elevated GEM events on June 8th and July 19th coincided with southwesterly winds, suggesting the transport of Hg from regional sources. Back

trajectories during the June 8th and July 19th events revealed several sources southwest of the sampling site, which included local sources (sewage treatment, electrical products production) and regional sources (metal production, sewage treatment, other urban cities). Hg emissions from nearby urban sources are potentially contributing to the elevated GEM event on July 19th, since an increase in pollutant (Hg and NO_x) concentrations, lack of wind, and clear skies indicate stable atmospheric conditions. Decreasing RGM/PHg<2.5 during an elevated GEM event on Oct. 20th coincided with easterly winds, and local sources east of the sampling site (metal production, sewage treatment) were identified by back trajectories and confirmed by wind directions measured by two weather stations in downtown Toronto.

- ***Correlation Analysis:*** Direct emissions are the sources of RGM in spring, summer and fall and photo-oxidation of GEM only becomes a major factor in the summer. RGM was correlated with O_3 during 2 elevated GEM events on May 26th and June 8th. RGM concentrations peaked during the noon hours in both events, indicating the oxidation of GEM to RGM by O_3. Nighttime RGM and O_3 peaks during the June 8th event indicate the potential transport of oxidizing air masses at night from distant sources, which is consistent with back trajectory, RGM/PHg<2.5, and wind analysis results. RGM and NO_x were correlated during 2 elevated GEM events on June 28th and July 19th, suggesting combustion processes, but diurnal NO_x trends were not consistent with vehicle emissions. Coal combustion is not likely a source of Hg in Toronto because RGM and SO_2 were not correlated in all the elevated Hg events; however, it does emit pollutants that can lead to the formation of ozone.

4.2 Significance of Findings

- The model results from this study suggested that metals production, sewage treatment and chemical products manufacturing contribute to atmospheric mercury in Toronto. The elevated Hg events in Toronto are attributed to emissions from regional point sources, photochemical processes involving ozone, and potentially urban sources near the sampling location that have not been identified or reported in the emissions inventory. These findings are significant because it provides some insight into sources that require more emissions control and pollution prevention measures. Metal processing plants were the top five emitters of Hg in Ontario in 2004 and since then, Canada Wide Standards on mercury emissions from base metal processing facilities have been implemented, which suggests that air pollution control technologies are needed. Although sewage treatment and chemical products manufacturing are not major emitters of Hg in Ontario, our data analysis have attributed these sources to atmospheric Hg in Toronto. This finding is significant because it has implications about the use and improper disposal of products containing mercury. Hg emissions from sewage treatment facilities likely came from the disposal of Hg-containing products into landfills, where the acidic leachate containing Hg is potentially brought to the wastewater treatment plant, or Hg discharges from hospitals, labs, dental offices, or industrial plants are ending up in the sewage system. Pollution prevention measures are needed to encourage recycling of Hg-containing products and prevent the discharge of mercury into the sewer system.

- The use of statistical and air quality models for Hg source identification in this study have led to several discussions about data and model uncertainties. The HYSPLIT back

trajectory model does not accurately simulate the wind patterns through downtown Toronto because of the resolution of the meteorological data used in this study. Finer spatial and temporal resolution meteorological data is essential to model pollutant transport through the boundary layer of an urban atmosphere and to identify urban sources near the sampling site that are potentially contributing to the mercury levels measured in downtown Toronto. In this study, an attempt was made to verify the back trajectories by examining wind directions measured at two weather stations in downtown Toronto. Correlations of model-predicted GEM and RGM concentrations obtained from another study were used to identify the production of RGM from direct emissions or oxidation of GEM by ozone. But studies have found that model-predicted and measured concentrations of GEM and RGM could differ by a factor of 1.5 and 10, respectively, which suggests the large variability in the correlations of model-predicted GEM and RGM concentrations. This finding emphasizes that GEM and RGM reactions and transport mechanisms need to be fully incorporated into atmospheric Hg models to conduct source identification studies.

- The PMF and PCA model extracted factors that cannot be characterized using NPRI emissions data from point sources. The NPRI emissions inventory does not report emissions data from urban sources that emit Hg (e.g., urban soils and pavement, use and disposal of fluorescent lamps and thermometers, fugitive emissions from buildings, traffic). These may be significant sources of Hg in Toronto, since only 3 major Hg point sources were within 100 km of the Toronto sampling site. Therefore, more research is needed to identify and quantify the Hg emissions from urban sources. To determine how

these sources affect Hg concentrations in the urban environment, future research might involve modeling the effect of traffic emissions on urban concentrations using a combined street canyon and Gaussian model, which has a spatial resolution ranging from ~20 km to a few meters (Mensink et al., 2008). The street canyon model simulates the impact of traffic emissions on a particular street, and the Gaussian model simulates the contributions of other sources on the rest of the urban environment (Mensink et al., 2008).

5. Appendix

5.1 Sample Calculations

5.1.1 Percent source contributions to receptor concentrations using PMF model outputs

Given:

Factor Profiles (F1 = factor 1, F2 = factor 2, …)

	F1	F2	F3	F4	F5	F6
GEM	0.1888	0.3464	0.0072	0.2019	3.9018	0.0013
PHg<2.5	0.1673	0	0	0	4.8421	18.641
RGM	0	0.2284	1.2701	1.6266	3.6144	8.2424
NO	7.2944	0.1252	0.0395	0.2299	0.0582	0
NO2	1.7676	16.184	0.0353	0.983	0.685	0.4764
NOx	9.1394	16.536	0.0011	1.3231	0.7654	0.4681
O3	0.0835	0.2304	0	22.634	0.5044	0
PM2.5	0.0113	0	7.1961	0	0.1844	0
SO2	0.0431	0.8367	0.5697	0.4423	0	0.3009

Source contributions for the first 3 samples/measurements (total # measurements for each pollutant = 3216)

Measurement #	F1	F2	F3	F4	F5	F6
1	0.0822	0.2747	0.5183	0.8931	1.4646	0.9739
2	0.2239	0.469	0.3844	0.6737	1.2594	0.8733
3	0.3996	0.321	0.0956	0.8421	1.6689	0.81

The PMF model equation (Equation (1)) is given by: $x_{ij} = \sum_{k=1}^{P} g_{ik} f_{kj}$

x_{ij} is the PMF model-predicted concentration of the jth specie at the receptor in the ith measurement; g_{ik} is the contribution of the kth factor on the ith measurement; f_{kj} is the mass concentration of the jth specie in the kth factor.

Thus for example, <u>factor 1's</u> model-predicted GEM concentration of the 1st measurement is

$x_{1,GEM} = g_{1,1} f_{1,GEM}$ = (0.0822)(0.1888 ng/m^3) = 0.0155 ng/m^3

<u>Factor 1's</u> model-predicted GEM concentration of the 2nd GEM measurement is

$x_{2,GEM} = g_{2,1} f_{1,GEM}$ = (0.2239)(0.1888 pg/m^3) = 0.0423 ng/m^3

Factor 1's model-predicted GEM concentration of the 3rd GEM measurement is

$x_{3,GEM} = g_{3,1} f_{1,GEM}$ = (0.3996)(0.1888 pg/m^3) = 0.0754 ng/m^3

Continue performing similar calculations for the rest of the GEM measurements (4 to 3216) to obtain factor 1's average GEM concentration. $[GEM]_{factor\ 1\text{-predicted, average}}$ = 0.1889 ng/m^3

Given, $[GEM]_{measured,\ average}$ = 4.647 ng/m^3

The percent source contribution of each factor to measured pollutant concentration is given by: $([pollutant]_{predicted}/[pollutant]_{measured})$ x 100%

Therefore, the average percent source contribution of factor 1 to GEM concentrations is (0.1889/4.647) x 100% = 4.1%

5.1.2 Calculation of NO_2/Hg, $PM_{2.5}$/Hg and SO_2/Hg at the source

Given, for example, the 2004 emissions data from NPRI for the OPG – Nanticoke facility (power generation):
NO_2 = 21,300 tons; $PM_{2.5}$ = 1,461 tons; SO_2 = 61,300 tons; total gaseous Hg = 134 kg

NO_2/Hg = 21,300 tons/134 kg = 159 tons NO_2/kg of Hg

$PM_{2.5}$/Hg = 1,461 tons/134 kg = 10.9 tons $PM_{2.5}$/kg of Hg

SO_2/Hg = 61,300 tons/134 kg = 458 tons SO_2/kg of Hg

5.1.3 Calculation of NO_2/Hg, $PM_{2.5}$/Hg and SO_2/Hg at the receptor/sampling site

Given, for example, the following pollutant concentrations at the sampling site during one of the elevated Hg event:
NO_2 = 28 ppb; $PM_{2.5}$ = 5.5 μg/m^3; SO_2 = 1 ppb; GEM = 5.560 ng/m^3; PHg<2.5 = 11.121 pg/m^3; RGM = 9.894 pg/m^3

Convert concentration units from ppb to $\mu g/m^3$ using the Ideal Gas equation at standard temperature and pressure (0^oC, 1 atm), since the Hg analyzer has referenced the concentrations to these conditions:

For NO_2 (M_{NO2} = 46 g/mol):

1 ppb of NO_2 = 1×10^{-9} mol NO_2/mol of air

Thus for every 1 ppb of NO_2 at 0^oC, 1 atm,

Mass concentration = PVM_{NO2}/RT

= (101,325 Pa)(1×10^{-9} mol NO_2/mol of air)(46 g/mol)/(8.314 J/mol K)(273.15 K)

= 2.052×10^{-6} g/m^3 = 2.052 $\mu g/m^3$

For SO_2 (M_{SO2} = 64 g/mol), every 1 ppb of SO_2 at 0^oC, 1 atm is equivalent to 2.856 $\mu g/m^3$ using the Ideal Gas Equation.

Thus, the mass concentration of NO_2 is (28 ppb)(2.052 $\mu g/m^3$/ppb) = 58 $\mu g/m^3$, and the concentration of SO_2 is (1 ppb)(2.856 $\mu g/m^3$/ppb) = 2.9 $\mu g/m^3$.

[Hg] = [GEM] + [PHg<2.5] + [RGM] = 5.560 ng/m^3 + (11.121 pg/m^3)/(1000 pg/ng) + (9.894 pg/m^3)/(1000 pg/ng) = 5.581 ng/m^3

Therefore, the NO_2/Hg, $PM_{2.5}$/Hg and SO_2/Hg at the receptor/sampling site are

NO_2/Hg = (58 $\mu g/m^3$)/(5.581 ng/m^3) = 10.3 μg of NO_2/ng of Hg

$PM_{2.5}$/Hg = (5.5 $\mu g/m^3$)/(5.581 ng/m^3) = 0.98 μg of $PM_{2.5}$/ng of Hg

SO_2/Hg = (2.9 $\mu g/m^3$)/(5.581 ng/m^3) = 0.52 μg of SO_2/ng of Hg

6. Reference List

Arain, M.A., Blair, R., Finkelstein, N., Brook, J.R., Sahsuvaroglu, T., Beckerman, B., Zhang, L., and Jerrett, M. (2007). The use of wind fields in a land use regression model to predict air pollution concentrations for health exposure studies. Atmospheric Environment 41, 3453–3464.

Asano, S., Eto, K., Kurisaki, E., Gunji, H., Hiraiwa, K., Sato, M., Sato, H., Hasuike, M., Hagiwara, N., and Wakasa, H. (2000). Acute inorganic mercury vapour inhalation poisoning. Pathology International 50, 169-174.

Bagnato, E., Aiuppa, A., Parello, F., Calabrese, S., D'Alessandro, W., Mather, T.A., McGonigle, A.J.S., Pyle, D.M., and Wängberge, I. (2007). Degassing of gaseous (elemental and reactive) and particulate mercury from Mount Etna volcano (Southern Italy). Atmospheric Environment 41, 7377–7388.

Bash, J.O., Miller, D.R., Meyer, T.H., and Bresnahan, P.A. (2004). Northeast United States and Southeast Canada natural mercury emissions estimated with a surface emission model. Atmospheric Environment 38, 5683-5692.

Biegalski, S.R., Landsberger, S., Hoff, R.M. (1998). Source-receptor modeling using trace metals in aerosols collected at three rural Canadian Great Lakes sampling stations. Journal of Air and Waste Management Association 48, 227.

Brinkman, G., Vance, G., Hannigan, M.P., and Milford, J.B. (2006) Use of synthetic data to evaluate positive matrix factorization as a source apportionment tool for $PM_{2.5}$ exposure data. Environmental Science and Technology 40, 1892-1901.

Brown, S.G., Frankel, A., and Hafner, H.R. (2007). Source apportionment of VOCs in the Los Angeles area using positive matrix factorization. Atmospheric Environment 41, 227-237.

Canadian Council of Ministers of the Environment (CCME) (2000). Canada-Wide Standards for mercury emissions. Retrieved May 14, 2008, from http://www.ccme.ca/assets/pdf/mercury_emis_std_e1.pdf

Canadian Council of Ministers of the Environment (CCME) (2006). Canada-Wide Standards for mercury emissions from coal-fired electric power generation plants. Retrieved May 14, 2008, from http://www.ccme.ca/assets/pdf/hg_epg_cws_w_annex.pdf

Capita.wustl.edu. (1999). PM data analysis workbook: Source Apportionment. Retrieved October 23, 2006 from http://capita.wustl.edu/PMFine/Workbook/PMTopics_PPT/WB_SourceAttr/Version2/sld001.htm

Chow, J. and Watson, J. (2002). Review of $PM_{2.5}$ and PM_{10} apportionment for fossil fuel combustion and other sources by the chemical mass balance receptor model. Energy & Fuels 16, 222-260.

Chow, J.C., Watson, J.G., Kuhns, H., Etyemezian, V., Lowenthal, D.H., Crow, D., Kohl, S.D., Engelbreeht, J.P., and Green, M.C. (2004). Source profiles for industrial, mobile, and area sources in the Big Bend regional aerosol visibility and observational study. Chemosphere 54, 185-208.

City of Toronto. (2006). Release of 2006 Census results age and sex population counts. Retrieved May 20, 2008, from http://www.toronto.ca/demographics/pdf/2006_age_and_sex_backgrounder_with_maps.pdf

Cobbett, F.D. and Van Heyst, B.J. (2007). Measurements of GEM fluxes and atmospheric mercury concentrations (GEM, RGM and Hgp) from an agricultural field amended with biosolids in Southern Ont., Canada (October 2004–November 2004). Atmospheric Environment 41, 2270-2282.

Davis, A., de Curnou, P., Eary, L.E. (1997). Discriminating between Sources of Arsenic in the Sediments of a Tidal Waterway, Tacoma, Washington. Environmental Science and Technology 31, 1985-1991.

Draxler, R.R. and Rolph, G.D. (2003). HYSPLIT (HYbrid Single-Particle Lagrangian Integrated Trajectory) Model access via NOAA ARL READY Website (http://www.arl.noaa.gov/ready/hysplit4.html). NOAA Air Resources Laboratory, Silver Spring, MD.

Dvonch, J.T., Graney, J.R., Keeler, G.J., Stevens, R.K. (1999). Use of elemental tracers to source apportion mercury in south Florida precipitation. Environmental Science and Technology 33, 4522-4527.

Eberly, S.I. (2005). EPA PMF 1.1 User's Guide. U.S. Environmental Protection Agency, Washington, DC, EPA/600/R-06/166 (NTIS PB2007-103431).

Ebinghaus, R., Kock, H.H., Temme, C., Einax, J.W., Lowe, A.G., Richter, A., Burrows, A.P., and Schroeder, W.H. (2003). Antarctic springtime depletion of atmospheric mercury. Environmental Science and Technology 36, 1238–1244.

Eckley, C.S. and Branfireun, B. (2008). Gaseous mercury emissions from urban surfaces: Controls and spatiotemporal trends. Applied Geochemistry 23, 369-383.

Edgerton, E.S., Hartsell, B.E., and Jansen, J.J. (2006). Mercury Speciation in Coal-fired Power Plant Plumes Observed at Three Surface Sites in the Southeastern U.S. Environmental Science and Technology 40, 4563-4570.

Elminir, H.K. (2007). Relative influence of air pollutants and weather conditions on solar radiation – Part 1: Relationship of air pollutants with weather conditions. Meteorology and Atmospheric Physics 96, 245-256.

Environment Canada. (2004a). Mercury and the Environment. Retrieved October 20, 2006 from http://www.ec.gc.ca/MERCURY/EN/index.cfm

Environment Canada. (2004b). National Climate Data and Information Archive. Retrieved August 10, 2007 from http://www.climate.weatheroffice.ec.gc.ca/climateData/hourlydata_e.html

Environment Canada. (2004c). National Pollutant Release Inventory. Retrieved April 10, 2008, from http://www.ec.gc.ca/pdb/npri/npri_home_e.cfm

Friedli, H.R., Radke, L.F., Prescott, R., Li, P.,Woo, J.-H., and Carmichael,G.R. (2004). Mercury in the atmosphere around Japan, Korea and China as observed during the 2001 ACEAsia field campaign: measurements, distributions, sources, and implications. Journal of Geophysical Research 109, D19 S25.

Gabriel, M.C., Williamson, D.G., Brooks, S., and Lindberg, S. (2005). Atmospheric speciation of mercury in two contrasting southeastern US airsheds. Atmospheric Environment 39, 4947–4958.

Garson, G.D. (2008). Factor Analysis. Retrieved May 14, 2008, from http://www2.chass.ncsu.edu/garson/pa765/factor.htm

Gebhart, K.A., Schichtel, B.A., and Barna, M.G. (2005). Directional biases in back trajectories caused by model and input data. Journal of the Air & Waste Management Association 55, 1649-1662.

Gochfeld, M. (2003). Cases of mercury exposure, bioavailability, and absorption. Ecotoxicology and Environmental Safety 56, 174–179.

Gustin, S., Coolbaugh, M.F., Engle, M.A., Fitzgerald, B.C., Keislar, R.E., Lindberg, S.E., Nacht, D.M., Quashnick, J., Rytuba, J.J., Sladek, C., Zhang, H., and Zehner, RE. (2003). Atmospheric mercury emissions from mine wastes and surrounding geologically enriched terrains. Environmental Geology 43, 339-351.

Hagreen, L.A. and Lourie, B.A. (2004). Canadian mercury inventories: the missing pieces. Environmental Research 95, 272-281.

Han, Y-J., Holsen, T.M., Lai, S-O., Hopke, P.K., Yi, S-M., Liu, W., Pagano, J., Falanga, L., Milligan, M., and Andolina, C. (2004). Atmospheric gaseous mercury concentrations in New York State: relationships with meteorological data and other pollutants. Atmospheric Environment 38, 6431–6446.

Heaton, R.W., Rahn, K.A., and Lowenthal, D.H. (1992). Regional Apportionment of Sulfate and Tracer Elements in Rhode Island Precipitation. Atmospheric Environment 26A, 1529-1543.

Honda, S., Hylander, L., and Sakamoto, M. (2006). Recent Advances in Evaluation of Health Effects on Mercury with Special Reference to Methylmercury – A Minireview. Environmental Health and Preventive Medicine 11, 171–176.

Hopke, P.K. (2003). Recent developments in receptor modeling. Journal of Chemometrics 17, 255-265.

Hylander, L.D. and Meili, M. (2005). The rise and fall of mercury: converting a resource to refuse after 500 years of mining and pollution. Critical Reviews in Environmental Science and Technology 35, 1-36.

Jaffe, D., Prestbo, E., Swartzendruber, P., Weiss-Penzias, P., Kato, S., Takami, A., Hatakeyama, S., and Kajii, Y. (2005). Export of atmospheric mercury from Asia. Atmospheric Environment 39, 3028-3038.

Keeler, G.J., Landis, M.S., Norris, G.A., Christianson, E.M., and Dvonch, J.T. (2006). Sources of mercury wet deposition in Eastern Ohio, USA. Environmental Science and Technology 40, 5874-5881.

Kim, K.H., and Kim, M.Y. (2001). The temporal distribution characteristics of total gaseous mercury at an urban monitoring site in Seoul during 1999-2000. Atmospheric Environment 35, 4253-4263.

Landis, M.S., Keeler, G.J., Al-Wali, K.I., and Stevens, R.K. (2004). Divalent inorganic reactive gaseous mercury emissions from a mercury cell chlor-alkali plant and its impact on near-field atmospheric dry deposition. Atmospheric Environment 38, 613–622.

Landis, M.S., Lewis, C.W., Stevens, R.K., Keeler, G.J., Dvonch, J.T., and Tremblay, R.T. (2007). Ft. McHenry tunnel study: Source profiles and mercury emissions from diesel and gasoline powered vehicles. Atmospheric Environment 41, 8711-8724.

Lee, J.H. and Hopke, P.K. (2006). Apportioning sources of $PM_{2.5}$ in St. Louis, MO using speciation trends network data. Atmospheric Environment 40, S360-S377.

Lee, P.H., Brook, J.R., Dabek-Zlotorzynska, E., and Mabury, S.A. (2003). Identification of the Major Sources Contributing to PM2.5 Observed in Toronto. Environmental Science and Technology 37, 4831-4840.

Lewis, C.W., Norris, G.A., Henry, R.C., and Conner, T.L. (2003). Source apportionment of Phoenix $PM_{2.5}$ aerosol with the UNMIX receptor model. Journal of Air and Waste Management Association 53, 325-338.

Lin, C.J., Pongprueksa, P., Lindberg, S.E., Pehkonen, S.O., Byun, D., and Jang, C. (2006). Scientific uncertainties in atmospheric mercury models I: Model science evaluation. Atmospheric Environment 40, 2911-2928.

Lindberg, S.E. and Stratton, W.J. (1998). Atmospheric mercury speciation: Concentrations and behavior of reactive gaseous mercury in ambient air. Environmental Science and Technology 32, 49-57.

Lindberg, S.E., Hanson, P.J., Meyers, T.P., and Kim, K.-H. (1998). Air/surface exchange of mercury vapor over forests—the need for a reassessment of continental biogenic emissions. Atmospheric Environment 32, 895-908.

Liu, B., Keeler, G.J., Dvonch, J.T., Barres, J.A., Lynam, M.M., Marsik, F.J., and Morgan, J.T. (2007). Temporal variability of mercury speciation in urban air. Atmospheric Environment 41, 1911-1923.

Lohman, K., Seigneur, C., Edgerton, E., and Jansen, J. (2006). Modeling Mercury in Power Plant Plumes. Environmental Science and Technology 40, 3848-3854.

Lynam, M.M. and Keeler, G.J. (2005). Automated speciated mercury measurements in Michigan. Environmental Science and Technology 39, 9253-9262.

Lynam, M.M. and Keeler, G.J. (2006). Source-receptor relationships for atmospheric mercury in urban Detroit, Michigan. Atmospheric Environment 40, 3144–3155.

Manolopoulos, H., Schauer, J.J., Purcell, M.D., Rudolph, T.M., Olson, M.L., Rodger, B., and Krabbenhoft, D.P. (2007a). Local and regional factors affecting atmospheric mercury speciation at a remote location. Journal of Environmental Engineering Science 6, 491-501.

Manolopoulos, H., Snyder, D.C., Schauer, J.J., Hill, J.S., Turner, J.R., Olson, M.L., and Krabbenhoft, D.P. (2007b). Sources of Speciated Atmospheric Mercury at a Residential Neighborhood Impacted by Industrial Sources. Environmental Science and Technology 41, 5626-5633.

Mensink, C., De Ridder, K., Deutsch, F., Lefebre, F., and Van de Vel, K. (2008). Examples of scale interactions in local, urban, and regional air quality modelling. Atmospheric Research, doi:10.1016/j.atmosres.2008.03.020, article in press.

Nacht, D.M., Sexauer Gustin, M., Engle, M.A., Zehner, R.E., and Giglini, A.D. (2004). Atmospheric Mercury Emissions and Speciation at the Sulphur Bank Mercury Mine Superfund Site, Northern California. Environmental Science and Technology 38, 1977-1983.

National Aeronautics and Space Administration (NASA) (2008). My NASA Data. Retrieved June 27, 2008, from http://mynasadata.larc.nasa.gov/data.html

Ontario Ministry of the Environment. (2004). Historical air quality pollutant data. Retrieved January 20, 2007, from http://www.airqualityontario.ca/

Ontario Ministry of the Environment. (2008). Ontario smog advisories for 2004. Retrieved March 15, 2007, from http://www.airqualityontario.com/press/advisories_2004.cfm

Paatero, P., and Hopke, P.K. (2003). Discarding or downweighting high-noise variables in factor analytic models. Analytica Chimica Acta 490, 277-289.

Pacyna, E.G., Pacyna, J.M., Steenhuisen, F., and Wilson, S. (2006). Global anthropogenic mercury emission inventory for 2000. Atmospheric Environment 40, 4048-4063.

Pallant, J. (2005). SPSS survival manual. 2nd Ed. Berkshire, UK: Open University Press. Chapter 15.

Pasquill, F. (1961). The estimation of the dispersion of windborne material. Meteorological Magazine 90, 33–49.

Pirrone, N., Costa, P., Pacyna, J.M., and Ferrara, R. (2001). Mercury emissions to the atmosphere from natural and anthropogenic sources in the Mediterranean region. Atmospheric Environment 35, 2997-3006.

Poissant, L., Pilote, M., Xu, X., and Zhang, H. (2004). Atmospheric mercury speciation and deposition in the Bay St. Francois wetlands. Journal of Geophysical Research 109, D11301.

Poissant, L., Pilote, M., Beauvais, C. Constant, P., and Zhang, H.H. (2005). A year of continuous measurements of three atmospheric mercury species (GEM, RGM and Hg_p) in southern Quebec, Canada. Atmospheric Environment 39, 1275–1287.

Ralston, N., Olson, E. and Wocken, C. (2005). Mercury Information Clearinghouse Quarter 5 – Mercury Fundamentals. Canadian Electricity Association.

Robinson, A.L., Subramanian, R., Donahue, N.M., Bernardo-Bricker, A., and Rogge, W.F. (2006). Source Apportionment of Molecular Markers and Organic Aerosols 1. Polycyclic Aromatic Hydrocarbons and Methodology for Data Visualization. Environmental Science and Technology 40, 7803-7810.

Rolph, G.D. (2003), Real-time Environmental Applications and Display sYstem (READY) Website (http://www.arl.noaa.gov/ready/hysplit4.html). NOAA Air Resources Laboratory, Silver Spring, MD.

Rutter, A.P., Schauer, J.J., Lough, G.C., Snyder, D.C., Kolb, C.J., Klooster, S.V., Rudolf, T., Manolopoulos, H., and Olson, M.L. (2008). A comparison of speciated atmospheric mercury at an urban center and an upwind rural location. Journal of Environmental Monitoring 10, 102-108.

Ryaboshapko, A., Bullock Jr., O.R., Christensen, J., Cohen, M., Dastoor, A., Ilyin, I., Petersen, G., Syrakov, D., Artz, R.S., Davignon, D., Draxler, R.R., and Munthe, J. (2007). Intercomparison study of atmospheric mercury models: 1. Comparison of models with short-term measurements. Science of the Total Environment 376, 228-240.

Schichtel, B. and Wishinski, P. (1996). HY-SPLIT and CAPITA Monte Carlo Model Back Trajectory Comparison. Retrieved May 15, 2008, from http://capita.wustl.edu/otag/reports/trajcomp/trajcomp.html

Schroeder, W.H. and Munthe, J. (1998). Atmospheric mercury–an overview. Atmospheric Environment 32, 809–822.

Sillman, S., Marsik, F.J., Al-Wali, K.I., Keeler, G.J., and Landis, M.S. (2007). Reactive mercury in the troposphere: Model formation and results for Florida, the northeastern United States, and the Atlantic Ocean. Journal of Geophysical Research 112, D23305.

Song, X. (2005). Studies of mercury species in the atmosphere in downtown Toronto. Master's Thesis Dissertation. Ryerson University, Toronto, Canada.

Southworth, G.R., Lindberg, S.E., Zhang, H., and Anscombe, F.R. (2004). Fugitive mercury emissions from a chlor-alkali factory: sources and fluxes to the atmosphere. Atmospheric Environment 38, 597-611.

Stamenkovic, J., Lyman, S., and Gustin, M.S. (2007). Seasonal and diel variation of atmospheric mercury concentrations in the Reno (Nevada, USA) airshed. Atmospheric Environment 41, 6662–6672.

Statistics Canada. (2006). 2006 Community Profiles. Retrieved May 20, 2008, from http://www12.statcan.ca/english/census06/data/profiles/community/Details/Page.cfm?B1=All&Code1=3520005&Code2=35&Custom=&Data=Count&Geo1=CSD&Geo2=PR&Lang=E&SearchPR=01&SearchText=Toronto&SearchType=Begins

St. Denis, M., Song, X., Lu, J.Y., and Feng, X.B. (2006). Atmospheric gaseous elemental mercury in downtown Toronto. Atmospheric Environment 40, 4016-4024.

Stein, A.F., Isakov, V., Godowitch, J., and Draxler, R.R. (2007). A hybrid modeling approach to resolve pollutant concentrations in an urban area. Atmospheric Environment 41, 9410-9426.

Streets, D.G., Hao, J., Wu, Y., Jiang, J., Chan, M., Tian, H., and Feng, X. (2005). Anthropogenic mercury emissions in China. Atmospheric Environment 39, 7789-7806.

Suarez, A.E., and Ondov, J.M. (2002). Ambient aerosol concentrations of elements resolved by size and by source: contributions of some cytokine-active metals from coal- and oil-fired power plants. Energy Fuels 16, 562-568.

Tabachnick, B.G., and Fidell, L.S. (2001). Using multivariate statistics. 4th Ed. NewYork: HarperCollins. Chapter 13.

Tang, S., Feng, X., Qiu, J., Yin, G., and Yang, Z. (2007). Mercury speciation and emissions from coal combustion in Guiyang, southwest China. Environmental Research 105, 175-182.

Temme, C., Blanchard, P., Steffen, A., Banic, C., Beauchamp, S., Poissant, L., Tordon, R., and Wiens, B. (2007). Trend, seasonal and multivariate analysis study of total gaseous mercury data from the Canadian atmospheric mercury measurement network (CAMNet). Atmospheric Environment 41, 5423-5441.

Turner, D.B. (1964). A diffusion model for an urban area. Journal of Applied Meteorology 3, 83–91.

Twigg, M.V. (2007). Progress and future challenges in controlling automotive exhaust gas emissions. Applied Catalysis B: Environmental 70, 2-15.

USEPA Office of Research and Development. (2007). EPA Positive Matrix Factorization 1.1 (EPA PMF 1.1). Model download from http://www.epa.gov/heasd/products/pmf/pmf.htm

Watkins, Marley. (2000). Monte Carlo Analysis. Retrieved July 20, 2007, from www.allenandunwin.com/spss.htm

Watson, J.G., Chow, J.C., and Fujita, E.M. (2001). Review of volatile organic compound source apportionment by chemical mass balance. Atmospheric Environment 35, 1567-1584.

Weast, R.C. and Selby, S.M. (1967). Handbook of Chemistry and Physics. 48th Ed. Cleveland, Ohio: Chemical Rubber Co.

Wong, C.S.C., Duzgoren-Aydin, N.S., Aydin, A., and Wong, M.H. (2006). Sources and trends of environmental mercury emissions in Asia. Science of the Total Environment 368, 649–662.

Zoras, S., Triantafyllou, A.G., and Deligiorgi, D. (2006). Atmospheric stability and PM10 concentrations at far distance from elevated point sources in complex terrain: Worst-case episode study. Journal of Environmental Management 80, 295–302.